

1V 83-25757

NASA CR 83098

CAPTURE OF LIQUID HYDROGEN BOILOFF WITH METAL HYDRIDE ABSORBERS

FINAL REPORT

PREPARED FOR

NATIONAL AERONAUTICS AND SPACE ADMINISTRATION

JOHN F. KENNEDY SPACE CENTER

CONTRACT NAS10-10625

WORK PERFORMED BY:

ERGENICS, INC

WYCKOFF, NEW JERSEY

April 1984

TABLE OF CONTENTS

	<u>Page No.</u>
LIST OF FIGURES	i
LIST OF TABLES	ii
ABSTRACT	iii
I. EXECUTIVE SUMMARY	1
II. INTRODUCTION	7
A. Background	7
B. Hydride Applications at KSC	8
C. Capture Demonstrations	11
III. APPROACH	12
A. Task 1 - System Performance Requirements	14
B. Task 2 - Hydride Alloy Selection	17
C. Task 3 - Hydride Container Design	31
D. Task 4 - Alloy/Container Design Verification Test	34
E. Task 5 - Hydride Alloy Manufacture	36
F. Task 6 - Container Construction and System Assembly	38
G. Task 7 - System Test	42
H. Task 8 - Report Preparation	45
I. Task 9 - Proof of Concept Demonstration & Project Review	45
IV. FULL SCALE SYSTEM	46
V. FINAL COMMENTS AND RECOMMENDATIONS	52
ACKNOWLEDGEMENTS	53
REFERENCES	54
APPENDIX	A-1

LIST OF FIGURES

<u>FIGURE NUMBER</u>		<u>PAGE NO.</u>
1	Cumulative Annual Boiloff at KSC	9
2	Off-loading Boiloff Rate Profile	11
3	Hydride and Boiloff Profile Comparison	16
4	Comparative Kinetics for Three Hydrides	18
5	Temperature Dependence of Kinetics for LaNi_5	19
6	Absorption Kinetics for $\text{LaNi}_{3.8}\text{Fe}_{1.2}$	19
7	Absorption Kinetics for $\text{LaNi}_{4.7}\text{Sn}_{0.3}$	20
8	Absorption Kinetics for LaNi_3Co_2	20
9	Reduced Pressure Kinetics of $\text{LaNi}_{4.9}\text{Al}_{0.1}$	21
10	Dynamic and Static Isotherms for $\text{LaNi}_{4.6}\text{Al}_{0.4}$	22
11	Static Isotherm for $\text{LaNi}_{3.8}\text{Fe}_{1.2}$	23
12	Static Isotherm for $\text{LaNi}_{4.7}\text{Sn}_{0.3}$	23
13	Dynamic Isotherm for $\text{CaNi}_{4.9}\text{Al}_{0.1}$	25
14	Dynamic Isotherm for $\text{LaNi}_3\text{-Co}_2$	26
15	Dynamic Isotherm for $\text{LaNi}_{4.7}\text{Al}_{0.3}$	27
16	Static Isotherm for $\text{LaNi}_{4.9}\text{Al}_{0.1}$	27
17	Dynamic Isotherm for LaNi_5	28
18	Static Isotherm for $\text{LaNi}_{4.6}\text{Al}_{0.4}$ T-88855-2	28
19	Dynamic Van't Hoff Diagrams for Five Alloys	29
20	Boiloff Capture Device Engineering Drawing	33
21	Small Coil Absorption Performance Curve	36
22	Isotherms for $\text{LaNi}_{4.6}\text{Al}_{0.4}$ T-88860-2	37
23	Static and Dynamic Van't Hoff Diagram for T-88860-2	37
24	Schematic of Demonstration Test Set-up	40
25	Hydrogen Boiloff Capture System	41

LIST OF FIGURES (CONTINUED)

<u>FIGURE NUMBER</u>		<u>PAGE NO.</u>
26	Remote Control Panel for KSC Demonstration	41
27	Balloon Poisoning Effect on Small Test Coil	41
28	Large Coil Absorption Performance	44
29	Boiloff Capture System Pictorial	48
30	Capture System Integration Schematic	49
31	LH ₂ Dewar Piping Diagram W/Capture Hook-up	50
32	Detail of Figure 31 Showing Hook-up Point	51

LIST OF TABLES

<u>TABLE NUMBER</u>	<u>DESCRIPTION</u>	<u>PAGE NO.</u>
1	Computer Run for 10 ft. dia., 10 ft. stack, 1% Hydride	3
2	Computer Run for 10 ft., dia., 10 ft. stack 1.2% Hydride	3
3	Computer Run for 12 ft., dia., 15 ft. stack 1.4% Hydride	4
4	Computer Program Listing	5 & 6
5	Tabulation of 36 Computer Runs	6
6	Candidate Alloy Properties	30
7	Small Test Coil Performance Data	35
8	Chemical Analysis for T-88855 and T-88860	36

ABSTRACT

Standard operating procedure at the Kennedy Space Center (KSC) for the Space Shuttle Program requires the storage and transfer of substantial quantities of liquid hydrogen (LH₂). Vaporized liquid, routinely lost during these transfer operations, is vented to the atmosphere or burned in the burn pond, and represents a significant fraction of the total hydrogen-fuel used for each launch. This report describes a procedure which uses metal hydrides to capture some of this low pressure (<1 psig) hydrogen for subsequent reliquefaction. Of the five normally occurring sources of boil-off vapor the stream associated with the off-loading of liquid tankers during dewar refill was identified as the most cost effective and readily recoverable. The design, fabrication and testing of a proof-of-concept capture device, operating at a rate that is commensurate with the evolution of vapor by the target stream, is described. Liberation of the captured hydrogen gas at pressures >15 psig at normal temperatures (typical liquefier compressor suction pressure) are also demonstrated. A payback time of less than three years is projected.

I. EXECUTIVE SUMMARY

A. Purpose

The volume of liquid hydrogen which will be used during the late 1980's by the Space Shuttle program at the Kennedy Space Center is expected to exceed 10 million gallons per year. Of this 10 million gallons only about 7 million will actually be used as propellant. The balance, over 3 million gallons per year, will be lost as boiloff in various transfer and storage operations at launch pads 39A and B.

The highest valued use for hydrogen boiloff identified during the preparation of the unsolicited proposal which led to this work was as feed stock for reliquefiers. Unfortunately, the boiloff rates during the intermittent loss periods are too high for economically sized equipment to reliquefy in "real time". The loss rates are also too high for conventional gas compressors and storage equipment to capture the boiloff vapor.

Metal hydride hydrogen absorbers are fast enough to capture the boiloff hydrogen during many of the loss episodes at LC-39. Hydrides are fairly expensive however, so the only losses which may be economically captured are those which are large and occur frequently. This leads to many cycles of use for the hydride and a large credit for hydrogen capture.

The most attractive use for hydrides identified in this program is for capturing the losses which occur during the transfer of liquid hydrogen from truck and rail cars. These "off-loading" operations will occur about 170 times per year⁽¹⁾. Other opportunities to capture boiloff are apparent which bring the total annual cycle number to about 200. Approximately 1.5 million gallons can be recovered from this source which will result in an annual savings >\$2 million (assuming \$1.50/gallon). At this rate of use, a metal hydride absorber will pay for itself in a few years of use (2-3 years depending on reliquefaction costs).

B. Approach

In the course of this program a "proof-of-concept" unit utilizing the unique characteristics of metal hydrides was designed, fabricated and tested. The

device was used with low pressure (atmospheric) hydrogen gas to demonstrate the technical feasibility of recovering hydrogen normally vented at the KSC.

C. Results

The test results indicate that a metal hydride capture/storage system:

- . Can absorb low pressure (<2.5 psig) hydrogen at a rate that is commensurate with the rapid boiloff of hydrogen vapor experienced during the LH₂ tanker "off-loading" operation.
- . Will interface with existing equipment at LC-39 with minimum impact on present operating procedures and be compatible with KSC safety practices.
- . Can release the stored hydrogen at normal temperatures and at pressures >2 atma for reliquefaction at a rate that is synchronized with the LH₂ delivery schedule.
- . Provides sufficient economic incentive to warrant consideration for further development of the concept at the KSC.

The tests confirmed the validity of the initial design configuration. A full-scale storage system (to absorb one-hour boiloff) will require 290,000 lbs of metal hydride. The hydride will be contained in 1-1/8 IN O.D. copper tubes with a flexible filter (gas distributor) on the axial center line for the full length of the coil. The tubes are spirally coiled with a minimum diameter of 2 feet and a maximum diameter of 10 feet. 73 coil layers are stacked in each of the five 10 ft. high vessels. See Tables 1-3 for three of the size options considered. Table 4 is a listing of the program that was used to generate the weight and size requirements of the full-scale system, and Table 5 is a compilation of thirty-six computer runs that represent the range of reasonable sizes.


```

***** INPUT DATA *****

TUBE DIAMETER = 1.125 IN          WALL THICKNESS = .05 IN
COIL DIAMETER -- MAXIMUM = 10 FT --- MINIMUM = 2 FT
SPACE BETWEEN COILS = .5 IN      BETWEEN LAYERS = .5 IN
HYDRIDE CAPACITY = 1 %           PACKING DENSITY = 60 %
MAXIMUM STACK HEIGHT = 15 FT     AXIAL FILTER OD .225 IN

***** LAYER TOTALS *****

NUMBER OF COILS = 29.54          COIL LENGTH = 556.5 FT
HYDRIDE WEIGHT = 764.16 LBS     HYDRIDE VOLUME = 1.824 FT3

***** SYSTEM TOTALS *****

COIL LAYERS PER STACK = 110     NUMBER OF STACKS REQUIRED = 4.04
TUBING LENGTH = 247605 FT       INTERNAL VOLUME = 1352.6 FT3

HYDRIDE VOLUME = 811.56 FT3 ---- 22.99 M3
HYDRIDE WEIGHT = 340000 LBS ---- 154545.45 KGS
HYDROGEN STORED = 3400 LBS ---- 1545.45 KGS
HYDROGEN STORED = 618181.82 SCF ---- 17512.23 SCM
HYDRIDE COST = 83090909          SYSTEM COST = 84327272
PAYBACK @ $1.8MM/YR = 2.4 YEARS

```

TABLE 1: Computer Run for 10 ft. diameter coil, 15 ft. stack height and 1% hydride storage capacity.

```

***** INPUT DATA *****

TUBE DIAMETER = 1.125 IN          WALL THICKNESS = .05 IN
COIL DIAMETER -- MAXIMUM = 10 FT --- MINIMUM = 2 FT
SPACE BETWEEN COILS = .5 IN      BETWEEN LAYERS = .5 IN
HYDRIDE CAPACITY = 1.2 %         PACKING DENSITY = 60 %
MAXIMUM STACK HEIGHT = 10 FT     AXIAL FILTER OD .225 IN

***** LAYER TOTALS *****

NUMBER OF COILS = 29.54          COIL LENGTH = 556.5 FT
HYDRIDE WEIGHT = 764.16 LBS     HYDRIDE VOLUME = 1.824 FT3

***** SYSTEM TOTALS *****

COIL LAYERS PER STACK = 73      NUMBER OF STACKS REQUIRED = 5.08
TUBING LENGTH = 206337 FT       INTERNAL VOLUME = 1127.16 FT3

HYDRIDE VOLUME = 676.3 FT3 ---- 19.16 M3
HYDRIDE WEIGHT = 283333.333 LBS ---- 128787.88 KGS
HYDROGEN STORED = 3400 LBS ---- 1545.45 KGS
HYDROGEN STORED = 618181.82 SCF ---- 17512.23 SCM
HYDRIDE COST = 82575757          SYSTEM COST = 83606000
PAYBACK @ $1.8MM/YR = 2 YEARS

```

TABLE 2: Computer Run for 10 ft. diameter coil, 10 ft. stack height and 1.2% hydride storage capacity.

```

***** INPUT DATA *****

TUBE DIAMETER = 1.125 IN          WALL THICKNESS = .05 IN
COIL DIAMETER -- MAXIMUM = 12 FT --- MINIMUM = 2 FT
SPACE BETWEEN COILS = .5 IN      BETWEEN LAYERS = .5 IN
HYDRIDE CAPACITY = 1.4 %         PACKING DENSITY = 60 %
MAXIMUM STACK HEIGHT = 15 FT     AXIAL FILTER OD .225 IN

***** LAYER TOTALS *****

NUMBER OF COILS = 36.92           COIL LENGTH = 911.57 FT
HYDRIDE WEIGHT = 1114.4 LBS       HYDRIDE VOLUME = 2.658 FT3

***** SYSTEM TOTALS *****

COIL LAYERS PER STACK = 110      NUMBER OF STACKS REQUIRED = 1.98
TUBING LENGTH = 176862 FT        INTERNAL VOLUME = 965.41 FT3

HYDRIDE VOLUME = 579.25 FT3 ---- 16.41 M3
HYDRIDE WEIGHT = 242857.143 LBS ---- 110389.61 KGS
HYDROGEN STORED = 3400 LBS ---- 1545.45 KGS
HYDROGEN STORED = 618181.82 SCF ---- 17512.23 SCM
HYDRIDE COST = $2207792          SYSTEM COST = $3090909
PAYBACK @ $1.8MM/YR = 1.72 YEARS

```

TABLE 3: Computer Run for 12 ft. diameter coil, 15 ft. stack height and 1.4% hydride storage capacity.

D. Recommendations

The next phase should include the following tasks:

- 1) The device fabricated in the performance of this contract should be tested using hydrogen from LH₂ boiloff.
- 2) An engineering analysis should be made of the various options available for hydrogen capture and storage for the purpose of identifying the most cost effective approach.
- 3) A single, full-scale component should be fabricated to operate in-situ at LC-39 to field test LH₂ boiloff capture capability.
- 4) Based on the results of all previous work, a full-scale system should be designed.
- 5) An RFQ should be issued to solicit bids for construction of the full-scale capture system.

```

1 HOME
10 DS = CHR* (4):I$ = CHR* (9)
15 REM
20 REM **** THIS IS COIL STACK ****
25 REM
30 REM THIS PROGRAM CALCULATES THE COIL LENGTH,VOLUME AND HYDROGEN CAPACITY F
OR A SPIRALLY WRAPPED LAYERED STACK
40 REM INPUTS REQUIRED ARE---- YD-HYDRIDE DENSITY, YC-HYDRIDE CAPACITY, PD-PA
CKING DENSITY, H-HYDROGEN TO BE ABSORBED
50 REM INPUTS REQUIRED ARE--- CD(1)-MAX COIL DIA, CD(2)-MINCOIL DIA, SH-MAX S
TACK HEIGHT, OD-TUBE OD, WT-TUBE WALLTHKNS, SP-SPACE BETWN COILS,FD-AXIAL FILTER
DIA, SL-SPACE BETWEEN LAYERS
60 REM OUTPUTS ARE--- TL(3)-TOTAL COIL LENGTH PER LAYER, TT-TOTAL COIL LENGTH
PER STACK, YW-HYDRIDE WEIGHT, SN-NUMBER OF STACKS RECD, NL-LAYERS PER STACK
70 INPUT "INPUT DIAMETER OF LARGEST COIL ";CD(1): INPUT "
INPUT DIAMETER OF SMA
LLEST COIL ";CD(2)
80 INPUT "
INPUT MAXIMUM STACK HEIGHT, FT ";SH: INPUT "
INPUT SPACE BETWEEN COI
LS, IN ";SP
90 INPUT "
INPUT SPACE BETWEEN LAYERS ";SL
100 INPUT "
INPUT TUBE OUTSIDE DIAMETER, IN ";OD: INPUT "
INPUT TUBE WALL THICK
NESS, IN ";WT
110 INPUT "
INPUT AXIAL FILTER OD, IN ";FD
120 INPUT "
INPUT HYDROGEN TO BE STORED, LBS ";H(3)
130 ID = OD - 2 * WT:Y = 1
140 P = OD + SP:NC(1) = (CD(1) / 2) / (P / 12):NC(2) = (CD(2) / 2) / (P / 12)
150 TH(1) = NC(1) * 2 * 3.14:TH(2) = NC(2) * 2 * 3.14
160 A = CD(1) / (2 * TH(1)):TL(1) = A * TH(1) ^ 2 / 2:TL(2) = A * TH(2) ^ 2 / 2:
TL(3) = TL(1) - TL(2)
170 INPUT "
INPUT HYDRIDE DENSITY, LB/FT3 ";YD: INPUT "
INPUT HYDRIDE CAPACITY,
% ";YC: INPUT "
INPUT PACKING DENSITY, % ";PD
180 NC(3) = NC(1) - NC(2):X = NC(3): GOSUB 780:NC(3) = X: PRINT "
TOTAL NUMBER
OF COILS PER LAYER = ";NC(3)
190 PRINT D$:"PR#1": PRINT I$:"U": PRINT I$:"80N"
200 ID = OD - 2 * WT
210 V = ((ID ^ 2 - FD ^ 2) * .7854 * TL(3)) / 144:YC = YC / 100:PD = PD / 100
220 YW(3) = H(3) / YC:YW(1) = V * PD * YD:H(1) = YW(1) * YC
230 X = TL(3): GOSUB 780
240 TL(3) = X:X = V: GOSUB 780
250 V = X:X = HY: GOSUB 780
260 HY = X:X = H: GOSUB 780
270 PRINT " "
280 PRINT TAB( 25);"***** INPUT DATA *****"
290 PRINT "
"
300 PRINT TAB( 5);"TUBE DIAMETER = ";OD;" IN"; TAB( 15);"WALL THICKNESS = ";WT
;" IN"
310 PRINT " "
320 PRINT TAB( 5);"COIL DIAMETER -- MAXIMUM = ";CD(1);" FT --- MINIMUM = ";CD
(2);" FT"
330 PRINT " "
340 PRINT TAB( 5);"SPACE BETWEEN COILS = ";SP;" IN"; TAB( 12);"BETWEEN LAYERS
= ";SL;" IN"
350 PRINT " "
360 PRINT TAB( 5);"HYDRIDE CAPACITY = ";YC * 100;" %"; TAB( 15);"PACKING DENSIT
Y = ";PD * 100;" %"
370 PRINT " "
380 PRINT TAB( 5);"MAXIMUM STACK HEIGHT = ";SH;" FT"; TAB( 11);"AXIAL FILTER O
D ";FD;" IN"

```

TABLE 4: Computer listing of program to calculate H₂ parameters of a spirally wrapped layered stack. (Continued on page 6.)

```

390 PRINT " ": PRINT " "
400 PRINT TAB( 25);"***** LAYER TOTALS *****"
410 PRINT " ": PRINT " "
420 PRINT TAB( 5);"NUMBER OF COILS = ";NC(3); TAB( 19);"COIL LENGTH = ";TL(3);
" FT"
430 X = YW(1): GOSUB 780
440 YW(1) = X
450 PRINT " "
460 PRINT TAB( 5);"HYDRIDE WEIGHT = "YW(1);" LBS"; TAB( 11);"HYDRIDE VOLUME =
";V * PD;" FT3"
470 NL = INT (SH * 12 / (OD + SL))
480 PRINT " ": PRINT " ": PRINT " "
490 PRINT TAB( 25);"***** SYSTEM TOTALS *****"
500 PRINT " ": PRINT " "
510 SN = (YW(3) / YW(1)) / NL
520 X = SN: GOSUB 780
530 SN(1) = X
540 PRINT TAB( 5);"COIL LAYERS PER STACK = ";NL; TAB( 12);"NUMBER OF STACKS RE
QUIRED = ";SN(1)
550 PRINT " "
560 TT = TL(3) * NL * SN: X = TT: GOSUB 780
570 TT = X
580 TV = V * NL * SN: X = TV: GOSUB 780
590 TV = X: TV(Y) = TV * PD: X = TV(Y): GOSUB 780
600 TV(Y) = X: TV(K) = TV(Y) / 35.3: X = TV(K): GOSUB 780: TV(K) = X
610 PRINT TAB( 5);"TUBING LENGTH = "; INT (TT);" FT": TAB( 14);"INTERNAL VOLUM
E = ";TV;" FT3"
620 PRINT " "
630 PRINT " "
640 PRINT TAB( 5);"HYDRIDE VOLUME = ";TV(Y);" FT3 ---- ";TV(K);" M3"
650 TK = YW(3) / 2.2: X = TK: GOSUB 780: TK = X
660 PRINT " "
670 PRINT TAB( 5);"HYDRIDE WEIGHT = ";YW(3);" LBS ---- ";TK;" KGS"
680 HW = YW(1) * NL * SN * YC: X = HW: GOSUB 780
690 HW = X
700 HK = HW / 2.2: X = HK: GOSUB 780: HK = X
710 CF = HW / .0055: X = CF: GOSUB 780
720 CF = X: CM = CF / 35.3: X = CM: GOSUB 780: CM = X
730 PRINT " "
740 PRINT TAB( 5);"HYDROGEN STORED = ";HW;" LBS ---- ";HK;" KGS"
750 PRINT " "
760 PRINT TAB( 5);"HYDROGEN STORED = ";CF;" SCF ---- ";CM;" SCM"
770 GOTO 800
780 X = ( INT ( X * 100 + .5) ) / 100
790 RETURN
800 CY = 14 * TK: X = CY: GOSUB 780: CY = X
810 CS = 1.4 * CY: X = CS: GOSUB 780: CS = X: PRINT " "
820 PRINT TAB( 5);"HYDRIDE COST = $"; INT (CY); TAB( 17);"SYSTEM COST = $"; IN
T (CS)
830 PB = CS / 1.8E6: X = PB: GOSUB 780: PB = X
840 PRINT " ": PRINT TAB( 5);"PAYBACK @ $1.8MM/YR = ";PB;" YEARS"
900 PRINT CHR$ (12): PRINT D$;"PR#0": END

```

TABLE 4: Continued

HYDRIDE CAPACITY, %	1.0			1.2			1.4																													
TUBING REQ'D, 10 ⁵ ft	3.40			2.83			2.43																													
HYDRIDE REQ'D, 10 ⁵ lbs	2.48			2.06			1.77																													
SYSTEM COST, 10 ⁶ \$	4.33			3.61			3.09																													
STACK HEIGHT, ft	10	15	20	10	15	20	10	15	20																											
COIL DIAMETER, ft	5	10	12	15	5	10	12	15	5	10	12	15	5	10	12	15	5	10	12	15																
VESSELS REQUIRED	28	6	4	3	18	4	3	2	14	3	2	4	3	23	5	4	2	15	3	15	12	3	2	1	20	4	3	2	13	3	2	13	10	2	15	1
PAYBACK TIME, years	2.40			2.00			1.72																													

TABLE 5: Computer projections for typical capture systems.

II INTRODUCTION

Several million gallons of liquid hydrogen boiloff losses are anticipated annually when the Space Shuttle program reaches full stride during the late 1980's unless means are found to prevent or reclaim this boiloff. The subject work tested the concept of using metal hydride hydrogen absorption systems to rapidly capture low pressure (<2 psig) gaseous hydrogen for subsequent reliquefaction at a greatly reduced rate.

A. Background

In 1978, Mr. Ed Snape of Ergenics and Dr. Gerry Golub of PRC Systems Service began discussing the possibilities for using metal hydrides to reduce hydrogen loss at the Kennedy Space Center (KSC). After a period of inactivity, the discussion was resumed between Greg Egan of Ergenics and Dr. Golub in April 1981.

In October 1981, Frank Lynch of Hydrogen Consultants, Inc., a subsidiary of Ergenics and Greg Egan traveled to KSC to meet with Jim Spears of NASA and others to explain hydride technology and begin a detailed discussion of possibilities for using the hydrogen normally lost during KSC operations.

The first possibility, which was considered in earlier discussions between Snape and Golub, was to fuel the buses which carry visitors on tours of the KSC. This presented a number of operational problems since NASA has developed hydrogen handling procedures and regulations which would need many modifications to permit the use of hydrogen in buses. The bus conversion would also involve a contractor (TWA) who operates the bus fleet for NASA.

In January of 1982, Egan and Matt Rosso of Ergenics met with Spears and others at KSC to present other possibilities for LH₂ boiloff utilization and reliquefaction. The possibilities considered were to:

1. Use steady-state boiloff to fuel a 50 KW Motor Generator (M-G) set.
2. Alter LH₂ delivery schedules so that transfer losses would be more uniform thus permitting the use of larger M-G sets producing 200-400 KW of electrical power.

3. Combine M-G sets with hydride technology (storage and compression) to augment the performance of a reliquefaction device.

These suggestions were well-received by NASA personnel. After additional preparation, Egan, Mark Golben and Rosso of Ergenics with Lynch of HCI returned to present a more detailed discussion of these concepts in April 1982. During this meeting it became clear that one of the most attractive possibilities for hydride use at KSC was the capture of large boiloff losses during transfer operations since this would complement the reliquefaction processes currently under consideration by NASA.

As the team of hydride experts became more familiar with the KSC Standard Operating Procedure (SOP) it became increasingly apparent that viable technical projects would require a sizeable effort to become familiar with the details of the hydrogen systems and with the people, procedures and regulations which control their use.

An unsolicited proposal was submitted in June, 1982 seeking a contract to demonstrate the technical feasibility of the most critical part of the hydrogen boiloff capture/reliquefaction concept - - rapid capture of the low pressure hydrogen vapor. In April, 1983 the subject contract (NAS10-10625) was awarded to Ergenics to perform the ten month program.

B. Hydride Applications at KSC

Most of the hydrogen vented at LC-39 is released in rapid bursts of short duration while cooling transfer plumbing or relieving pressure. It is uneconomical to install liquefiers large enough, or to use conventional gas compression and storage devices, to counter these losses. Metal hydrides, however, are capable of rapidly absorbing hydrogen gas at low pressures and normal temperatures and storing the captured gas until an economically sized liquefier can return it to the storage tank as liquid.

Figure 1 shows the cumulative loss estimate during one year of operation. At the bottom of the graph the relatively small stable boiloff is shown.

All of the reliquefaction schemes under consideration at NASA have the capability of capturing the stable boiloff so no hydrides are necessary for that purpose.

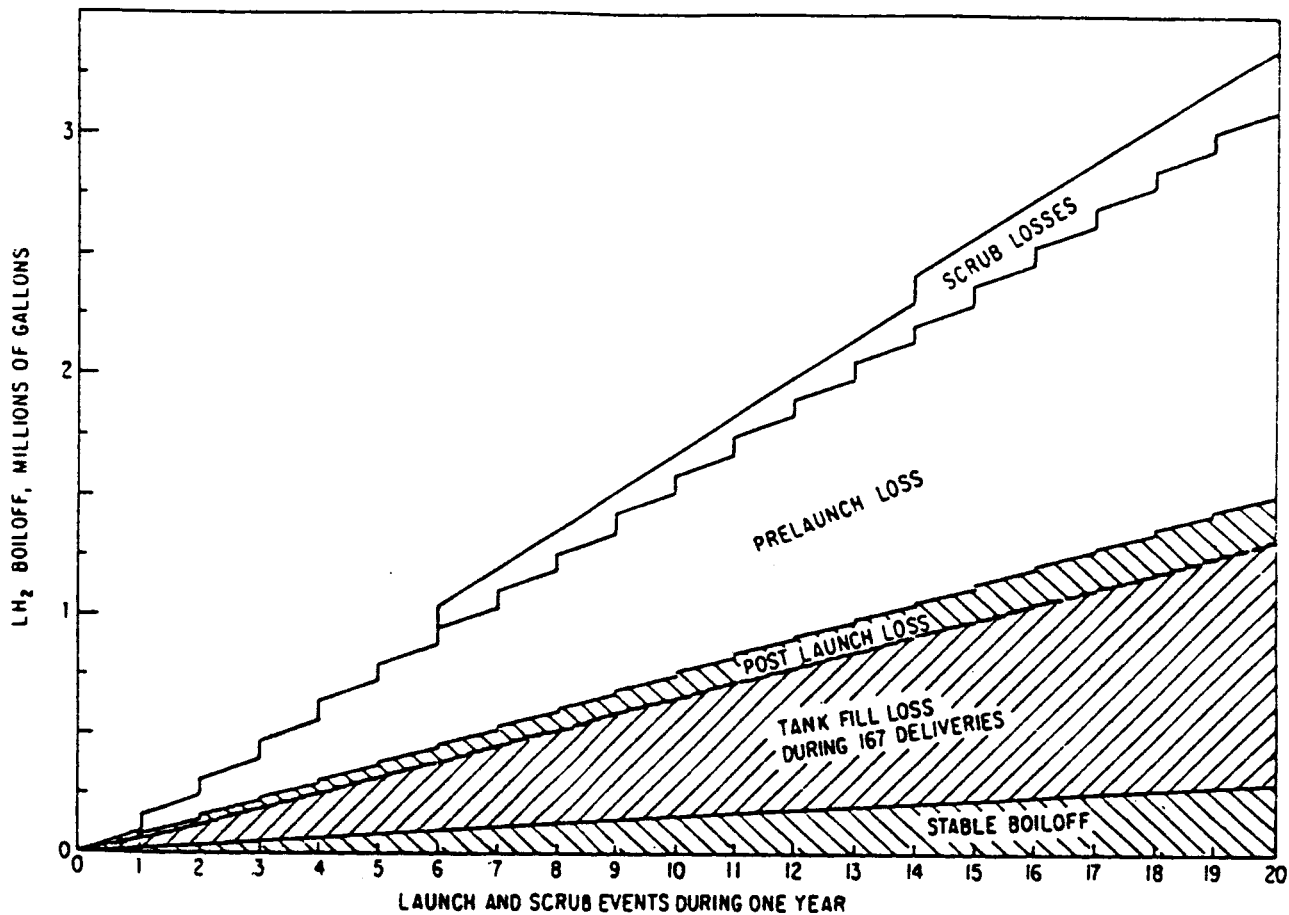


Figure 1: Cumulative boiloff losses during one year. Capturable losses are shown as cross-hatched area.

The region just above the steady-state boiloff line in Figure 1 represents the cumulative loss from truck and railcar deliveries of liquid hydrogen. Over one million gallons will be lost each year during these short (1.0 hour) LH₂ delivery periods.

The contribution of the pre-launch, post-launch and scrub losses represents more than 50% of the total boiloff; but hydrogen from these sources is not readily recoverable since they are too intimately associated with shuttle launch operations. Hydrogen vapor generated during the "pre-launch" operation is the largest single source of vented vapor. This hydrogen is vented at the Space Shuttle during the cooldown and filling of its external tanks (ET's), where as much as

250,000 gallons are lost during the refueling operation. The "post-launch" losses result from blow-down of the fill line which transports liquid hydrogen from the LH₂ storage dewar to the launch pad. The pressurized contents of this line is typically drained back to the dewar until pressures are equalized. The residual, low-pressure, hydrogen is then sent to the burn pond where it is ignited. 8000 gallons are flared for each launch episode which may be recoverable in the future when confidence in the capture system has been established. Capture of losses resulting from scrubbed missions, although large (100,000 gallons), are not cost effective since they are infrequent, unpredictable and too intimately associated with shuttle launch operations.

The present feeling at the KSC is that it is preferable to vent the hydrogen from the above three sources rather than risk over-pressurizing the external liquid hydrogen tank by preventing the free flow of hydrogen boiloff. In this study, we, therefore, addressed only the capture of hydrogen from the two remaining sources; the daily, stable boiloff and the LH₂ tanker off-loading losses.

During the transfer of hydrogen from the liquid hydrogen delivery trucks to the pad storage tank, approximately 10% of the fuel is lost. Five trucks arrive at the site, each with 13,000 gallons of LH₂. The hydrogen boiloff available for capture was estimated by NASA personnel to be about 6,500 gallons. "First-hand" observation of the off-loading procedure by Ergenics personnel and a fundamental modeling analysis conducted during the course of this program indicate that only 6,000 gallons are lost during this operation.

It was assumed, as shown in Figure 2, that the largest fraction of this hydrogen was boiloff produced during cooling of the transfer piping. In reality, the results of the study portion of this program show that the greatest contribution to boiloff is made by flashing of the liquid as the pressure decreases from the tanker transfer pressure (20-25 psig) to the dewar storage pressure (2.5 psig). See Appendix A(2). The time scale of Figure 2 is based on the NASA estimate of 1.5 hour total delivery period, with 1/2 hour of actual LH₂ transfer to the pad storage tank. Two "off-loadings" witnessed by Ergenics personnel required only one hour with LH₂ being transferred to the dewar for the entire period. The boiloff rate was more controlled than was originally anticipated with vapor being vented to the

atmosphere at a fairly uniform rate. The expected initial rapid discharge of vapor, as the transfer line is cooled to LH₂ temperatures, was not evident; and based upon the modeling study is not a significant contributor to the total boiloff. The dotted line on Figure 2 is more representative of the actual boiloff rate.

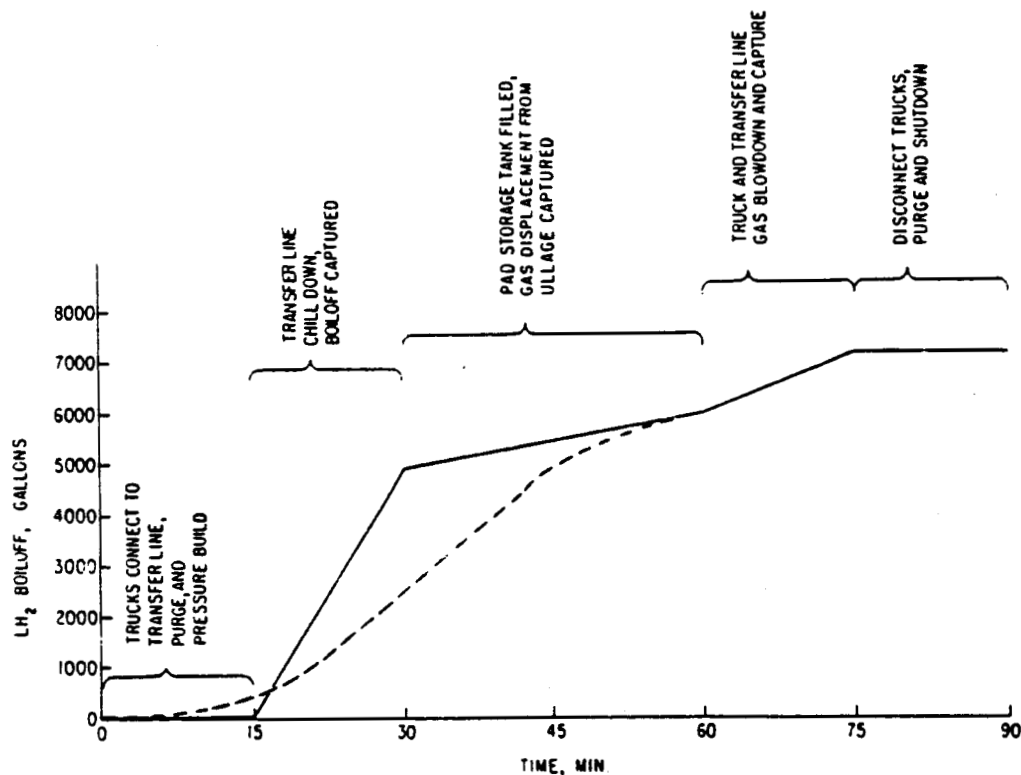


FIGURE 2: Estimated boiloff profile during a tank fill event.

C. Capture Demonstration

Capture of this vapor is not readily accomplished by normal means because of the extremely high mass flow-rate (>10,000 SCFM) and low pressure (<2.5 psig). Certain low pressure metal hydrides operating near ambient temperatures can absorb hydrogen very rapidly and well below atmospheric pressure. In the course of this work a proof-of-concept and a field test device were fabricated to demonstrate the rapid absorption of low pressure hydrogen. The body of this report contains a description of the device, the test results and recommendations for additional work culminating in the implementation of a full-scale capture/reliquefaction system at the KSC.

III. APPROACH

The approach is described in Section 4.0 TECHNICAL REQUIREMENTS section of the original Statement of Work, which follows:

4.0 TECHNICAL REQUIREMENTS

4.1 The effort will include the following tasks:

4.1.1 Task 1 - System Performance Requirement

The project team will meet with KSC personnel in order to study and specify the following boiloff capture design criteria:

4.1.1.1 Pad Storage Tank Fill Operation Boiloff:

Pressure

Temperature

Flow

Time Allotment

4.1.1.2 Hydride Capture Unit to Liquefier Transfer:

Pressure

Flow

Time Allotment

4.1.2 Task 2 - Hydride Alloy Selection

Based on the results of Task 1, one or more hydride alloys will be specified. Preliminary estimates of thermal ballast fraction, heat capacity, thermal conductivity, and heats of formation will be made.

4.1.3 Task 3 - Hydride Container Design

The hydride alloy selected in Task 2 and the performance requirements of Task 1 will be used as inputs to the design of a suitable container which must provide for ample gas flow means for heating and/or cooling and for control of powder expansion.

4.1.4 Task 4 - Alloy/Container Design Verification

A small batch of one or more alloys selected in Task 2 will be formed and inserted in a small-scale container representative of the design created in Task 3. The assembled unit will be tested on a Sieverts apparatus to verify performance.

4.1.5 Task 5 - Hydride Alloy Manufacture

The selected hydride alloy, verified in Task 4, will be formed in a quantity sufficient for the construction of a proof-of-concept boiloff capture unit.

4.1.6 Task 6 - Container Construction and System Assembly

The basic container design verified in Task 4, will be followed in constructing the proof-of-concept boiloff capture unit. The hydride alloy will be inserted, and readied for performance testing.

4.1.7 Task 7 - System Test

The completed boiloff capture unit will undergo a series of tests representative of the KSC pad storage tank transfer operations, specified in Task 1.

4.1.8 Task 8 - Report Preparation

A final project report will be prepared, detailing the design and performance of the boiloff capture unit. The report will also include the proposed future work statement and discussion of a full-scale system design for LC-39.

4.1.9 Task 9 - Proof-of-Concept Demonstration and Project Review

The complete boiloff capture unit will be shipped to KSC and demonstrated to key personnel. While the demonstration is being performed, it will be reviewed by the NASA project team who will notify interested parties at KSC who want to witness the demonstration.

The task sequence will be used as a format for the technical discussion.

A. Task 1 - System Performance Requirements

It became apparent during discussions with NASA and EG&G personnel that very little "hard" data existed concerning hydrogen vapor mass-flow-rates. It was also recognized that to attempt to make definitive measurements would be a major undertaking. We, therefore, agreed to base the engineering design of the test unit on whatever subjective information could be compiled as well as projections generated by computer modeling from first principles. Two liquid off-loadings were viewed by Ergenics personnel and some subjective measurements made. The estimated vapor flow-rates, based on these data, agreed very well with projections made by independent consultants working from engineering drawings of the LC39A LH₂ Storage Area (See Appendix A). The drawings and whatever other data were available were supplied by the NASA Technical Representative. The peak and

average hydrogen flow-rates were taken to be 10,650 and 10,300 SCFM (58.6 and 56.6 Lb/Min) respectively. It was also determined by thermodynamic analysis that the temperature of the gas entering the recovery unit will be from 35 to 85°K for capture line lengths up to 500 feet long. The relatively small temperature increase is attributed to the high linear velocity of the gas and, consequently, short residence time. The sensible heat capacity of the cold vapor will assist in the removal of the exothermic heat of reaction which is generated as the hydrogen is absorbed by the hydride.

In practice, the delivery trucks undergo a pressure building step in order to force the liquid through the transfer plumbing. The pressure within the truck's dewar is increased to 20-25 psig by vaporizing some of the liquid in an external heat exchanger. The pressure is maintained on the liquid until the truck's tank has discharged all of its LH₂. The first liquid to enter the transfer line plumbing boils away until cryogenic temperatures are reached.

After the transfer line has been chilled to allow liquid flow, the second opportunity for hydrogen capture occurs. As the pad storage tank is filled, the cold, gaseous hydrogen in the tank's ullage is displaced and vented. This gas is available for capture during the entire 1 hour fill period. After transfer, the high pressure gaseous hydrogen which remains in the trailers is vented before the trucks depart and is, therefore, available for capture during the latter stage of the delivery cycle.

The shape of the LH₂ boiloff profile, shown in Figure 2, is quite similar to the shape of a hydride charging profile, as shown in Figure 3. Both curves are shown together in order to illustrate their similar characteristics of initially high flowrates followed by a period of lower flowrates. The hydride charging profile is taken from laboratory data for a hydride with an absorption pressure of 0.5 atmospheres absolute at 25°C and an applied hydrogen pressure of 1 atmosphere absolute. The dotted line represents the more representative hydrogen boiloff rate as measured during this work. The actual capture mission is less demanding than originally anticipated, as the slope of the dotted curve indicates.

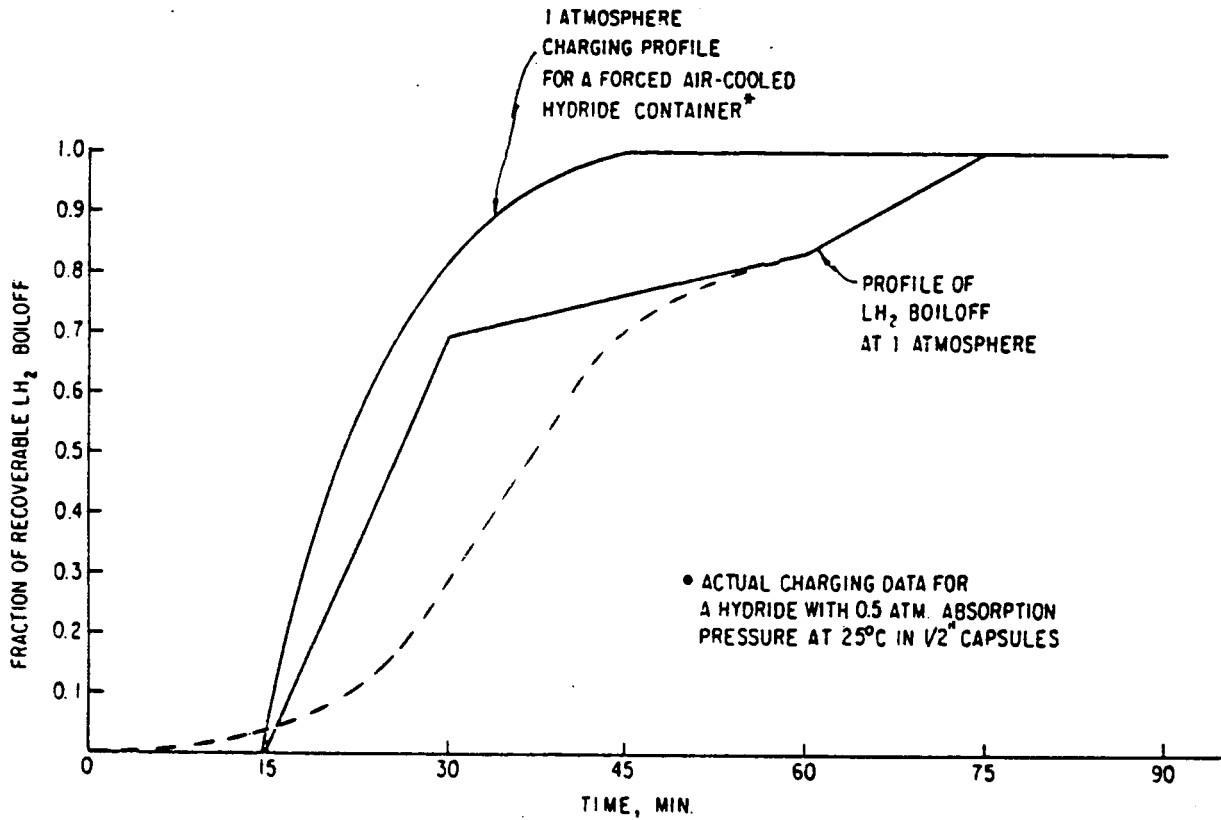


FIGURE 3: Comparison between the estimated boiloff loss profile and a hydride charging profile shows the feasibility of boiloff capture.

The parameters used for the design of the full-scale recovery system follow:

Hydrogen flow-rate (PEAK)	10,600 SCFM
Hydrogen storage capacity	3400 lbs. (620,000 SCF)
Cold water temperature/ flow-rate	20°C(68°F)/400 GPM for a 10°C (18°F) Rise
Hot water temperature/ flow-rate	80°C(176°F)/40 GMP for a 10°C (18°F) Rise
Maximum vessel diameter/height	15 ft/20 ft
Tubing diameter/wall thickness	1.125 in/0.050 in
Axial filter OD	0.225 in
hydride packing density	60%

B. Task 2 - Hydride Alloy Selection

The critical criteria that impact alloy selection will be discussed for each alloy considered. They include:

- . Hydrogen absorption capacity
- . Chemical kinetics
- . Dynamic hysteresis
- . Isotherm slope
- . Dynamic absorption plateau pressure <0.4 atma at 25° C
- . Alloy components availability
- . Dynamic desorption plateau pressure >2 atma at 75° C

DEFINITIONS

- . Hydrogen Absorption Capacity is the amount of hydrogen that can be reversibly stored in a metal hydride and is usually given as weight per cent of the metal, $(W_{H_2}/W_{Hydride}) \times 100$.
- . Chemical Kinetics is a measure of the time required for a hydrogen molecule to attach to the metal surface, dissociate into two H⁺ ions and be absorbed into the crystal lattice of the metal. Ideally the chemical kinetic rate is measured independently from heat transfer effects; but can have a measurable influence on the effective hydrogen absorption rate. Figure 4 depicts the absorption rate to 50% of full capacity for three different alloys. Differences greater than an order of magnitude are attributed to the inherent chemical kinetics for each alloy. These curves were generated at Ergenics under contract to Sandia National Laboratories in Albuquerque, New Mexico⁽³⁾. Figures 5-9, also taken from the Sandia final report, present the measured wide range of absorption rates for some of the alloys considered. Figures 5 and 6 depict the typical variation in kinetic rates as a function of temperature. Even small additions of aluminum seem to slow the chemical kinetic rate and increase its sensitivity to temperature change. This result makes it imperative that we know the temperature of the hydrogen vapor entering

the boiloff capture vessel. The effect of alloying elements, other than aluminum, is evident when Figures 7-9 are compared. Data are not available for $\text{LaNi}_{4.6}\text{Al}_{0.4}$; but reliable extrapolations can be made from the information presented here.

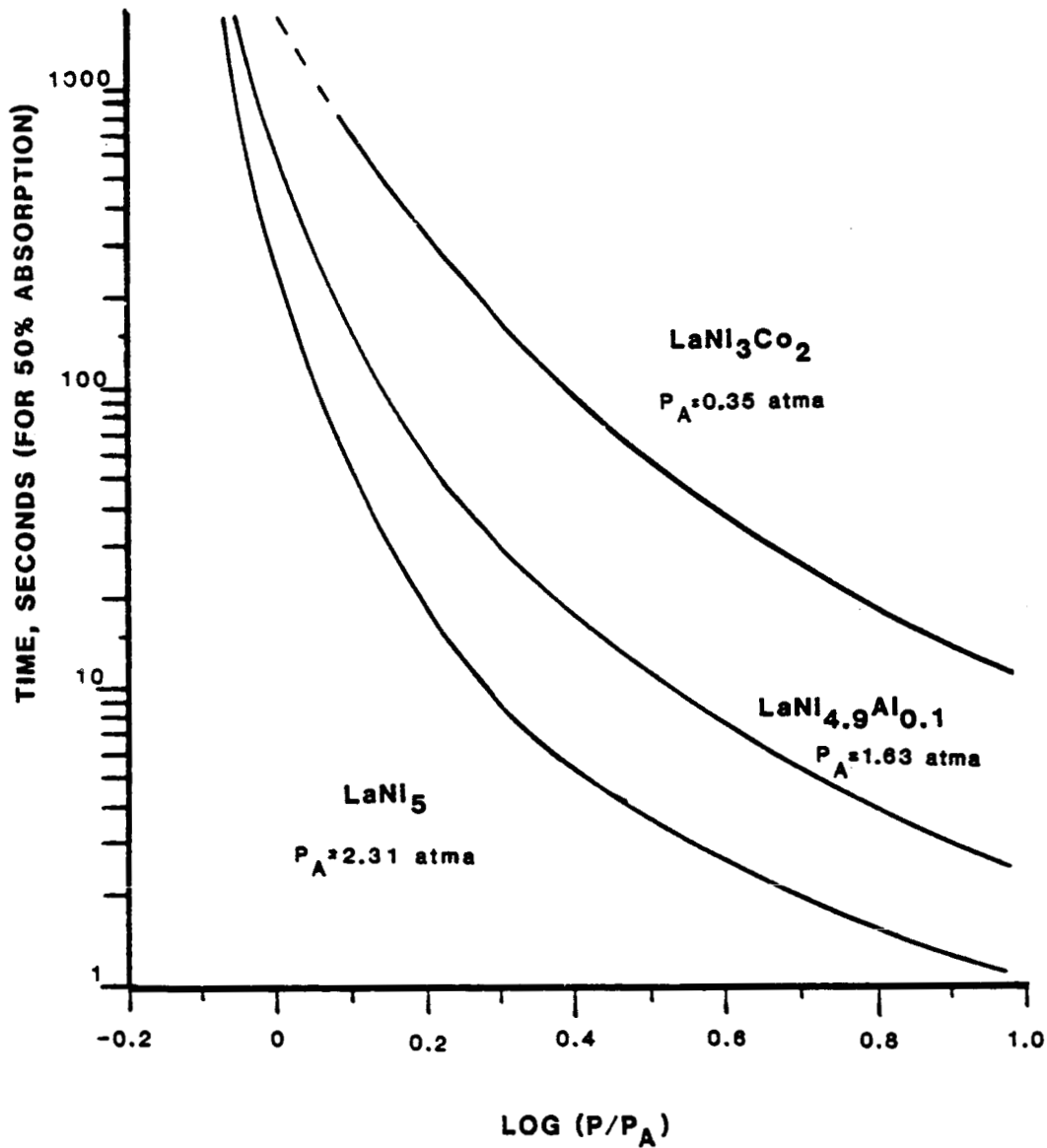


FIGURE 4: Absorption rate to 50% of full hydrogen capacity for three AB_5 alloys. Ref. 3

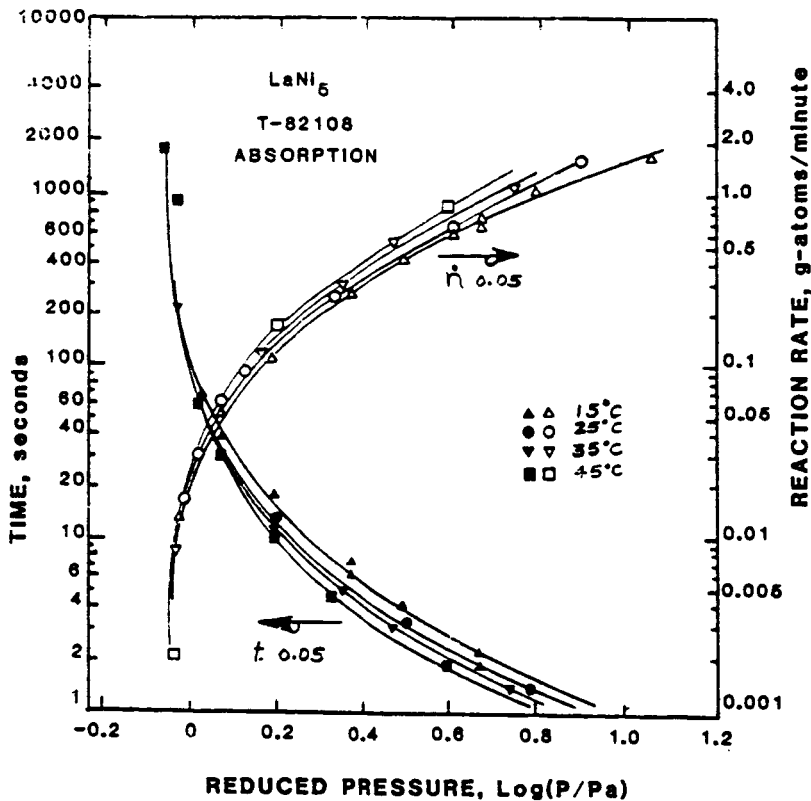


FIGURE 5: Comparison based on reduced pressure of LaNi_5 absorption kinetic data showing the rate and time to 0.05 g-atom H reacted at all pressures and temperatures tested ($\sim 0.5 \text{ H/M}$). Ref. 3.

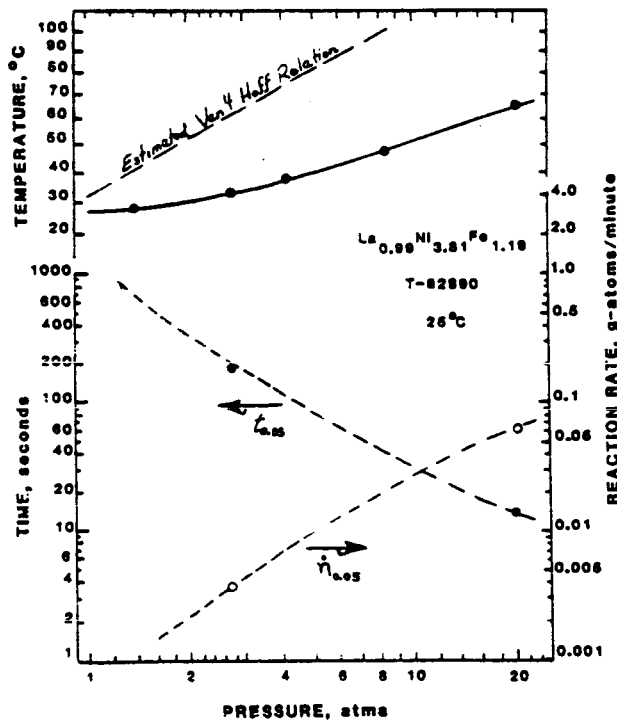


FIGURE 6: Summary of absorption kinetic data at 25°C showing the maximum temperature excursion as well as the reaction rate and time at 0.05 g-atoms hydrogen reacted ($\sim 0.5 \text{ H/M}$). Ref. 3.

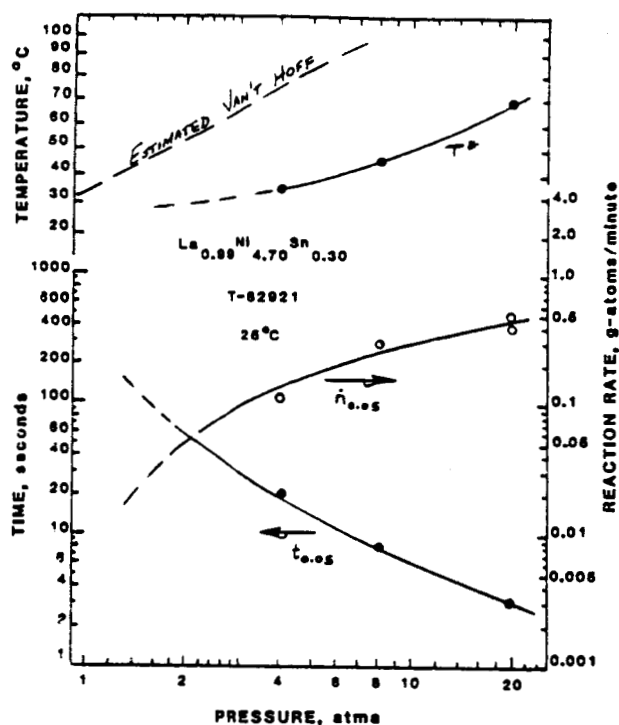


FIGURE 7: Summary of absorption kinetic data at 25°C showing the maximum temperature excursion as well as the reaction rate and time at 0.05 g-atoms hydrogen reacted ($\sim 0.5\text{H/M}$). Ref. 3.

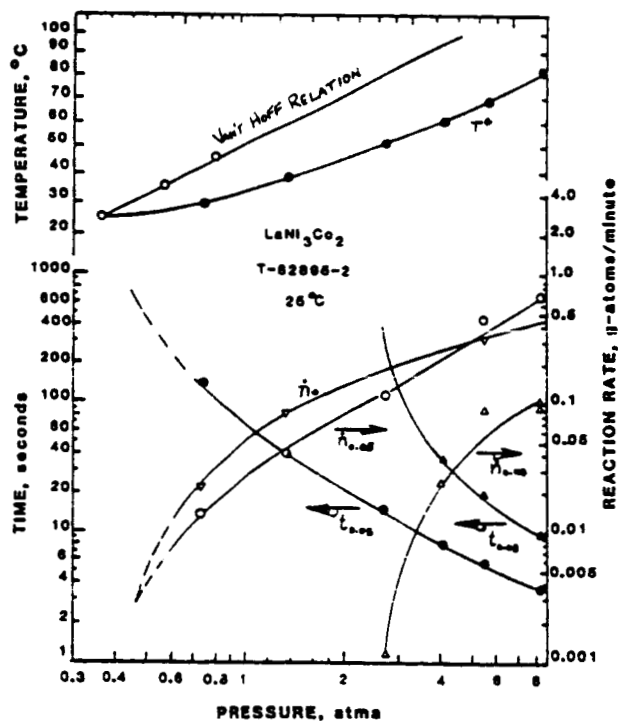


FIGURE 8: Summary of LaNi_3Co_2 absorption kinetic data at 25°C showing the maximum temperature excursion as well as the reaction rate and time parameters. Ref. 3.

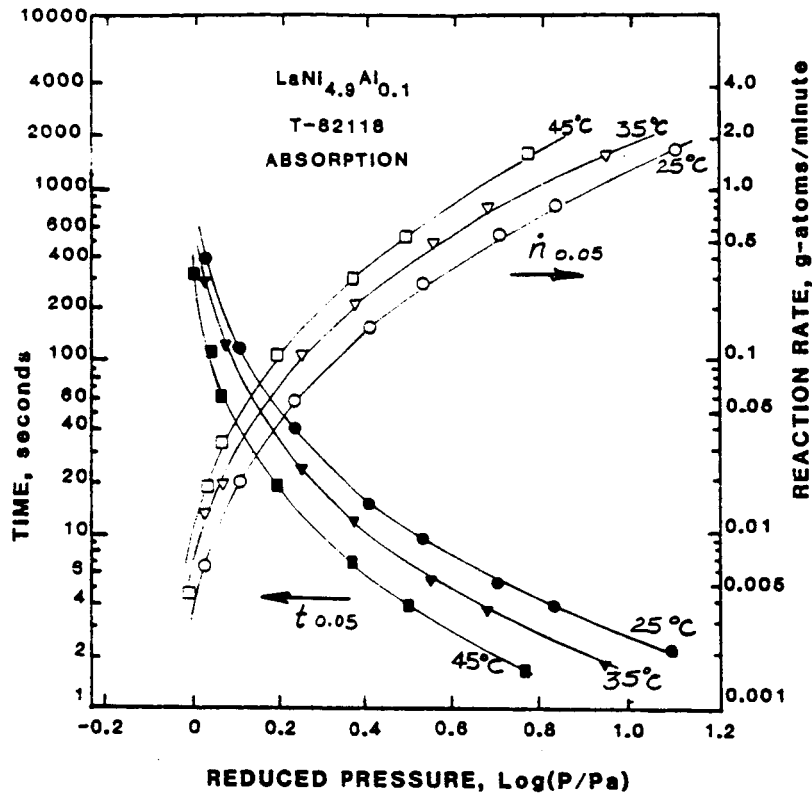


FIGURE 9: Comparison based on reduced pressure of $\text{LaNi}_{4.9}\text{Al}_{0.1}$ absorption kinetic data showing the rate and time to react 0.05 g-atom H at all pressures and temperatures tested (~ 0.5 H/M) Ref. 3.

- Dynamic Hysteresis - is the difference between the absorption and the desorption plateau pressure for a particular alloy while in the transient mode. The plateau pressures are significantly different for different hydrogen mass flow-rates. The desorption and absorption plateaus are depressed and raised respectively when compared with its equilibrium isotherm, as can be seen in Figure 10. For applications, such as the one being considered here, where hydrogen flow-rates are extremely rapid, the system design must be based upon dynamic values. Because the magnitude of this loss is an inherent characteristic of each hydride formulation, it is important to consider it when evaluating alloys for any application.
- Isotherm Slope - some hydrides, such as $\text{LaNi}_{3.8}\text{Fe}_{1.2}$ (Figure 11) and $\text{LaNi}_{4.7}\text{Sn}_{0.3}$ (Figure 12), exhibit a sloping plateau which has a profound effect on a hydride's applicability. For example, the tin substituted hydride (Figure 12) has a plateau that slopes from 0.15 to 1.5 atma at

25°C which makes it totally unsuitable even though its other characteristics (capacity and hysteresis) are acceptable.

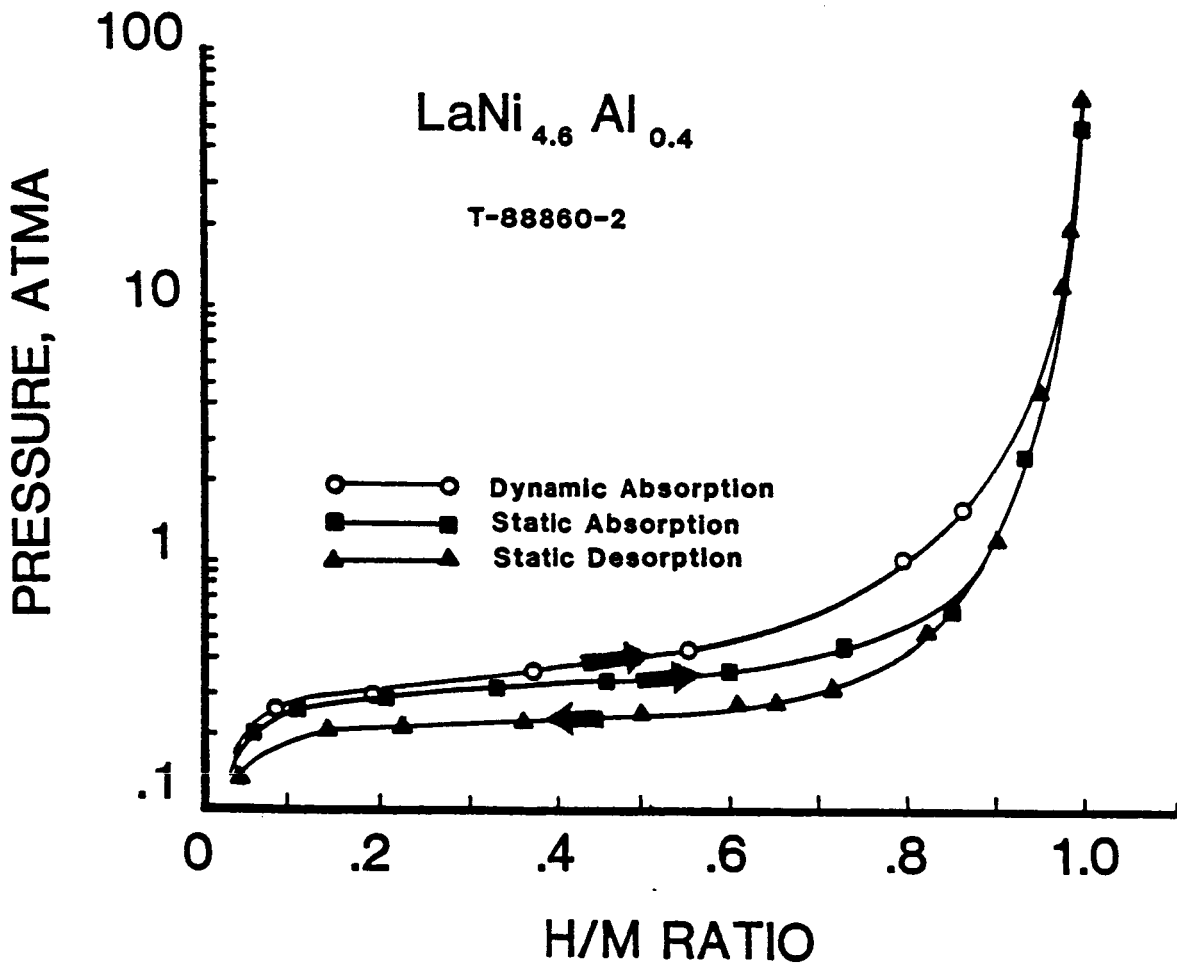


FIGURE 10: Static and dynamic 25°C isotherms for LaNi_{4.6}Al_{0.4}. Heat #T-88860-2.

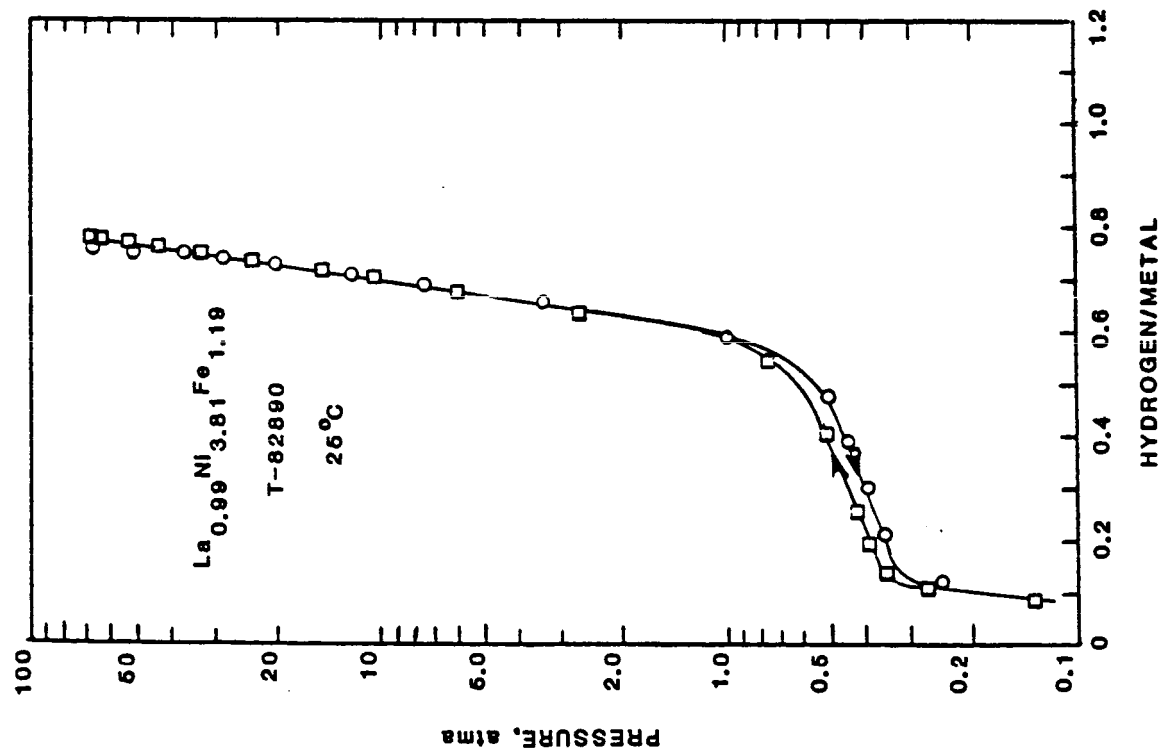


FIGURE 11: Static 25°C isotherms for as-cast $\text{LaNi}_{3.8}\text{Fe}_{1.2}$.

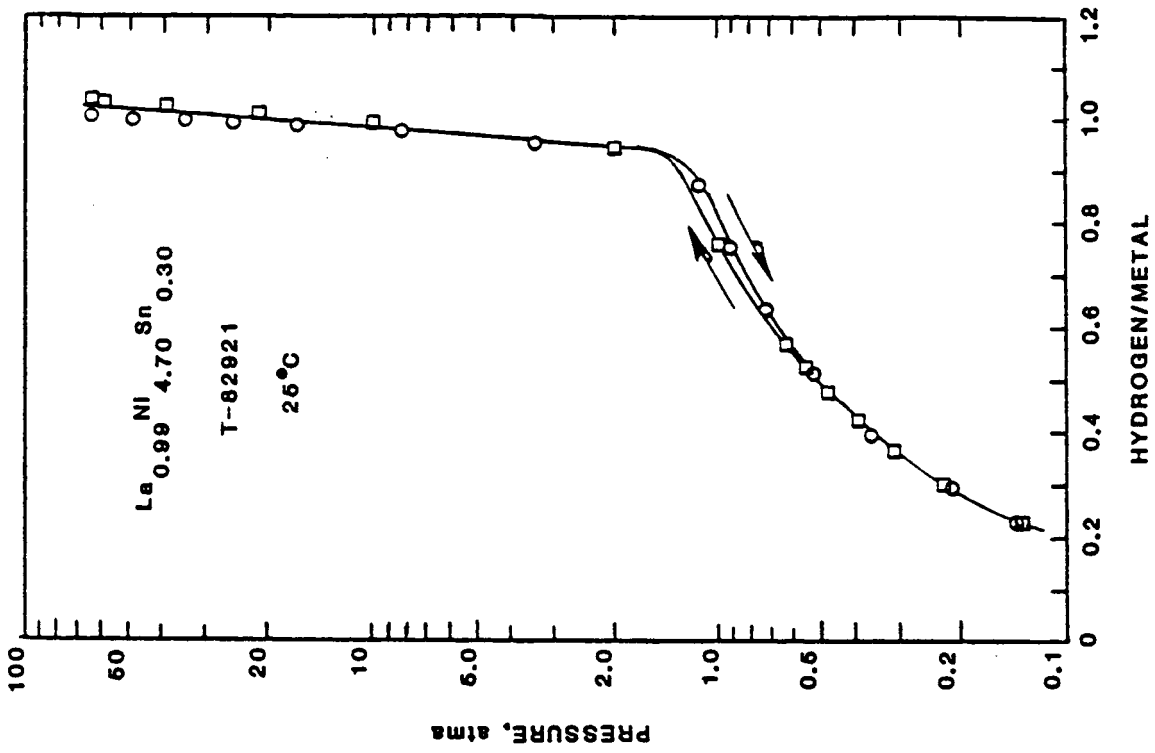


FIGURE 12: Static 25°C isotherms for as-cast $\text{LaNi}_{4.7}\text{Sn}_{0.3}$.

- Dynamic Absorption Plateau Pressure - is a primary aspect to be considered since the greater the pressure difference between the charging hydrogen stream and the hydride's absorption plateau, the greater will be the absorption rate. We, therefore, want this value to be as low as possible at normal temperatures (<0.4 atma at 25° C).
- Availability of Alloy Components - while not a major concern, should be addressed when making a hydride selection. The use of rare, expensive or sensitive materials must be avoided particularly where large quantities of hydride are to be used. Of the five candidates considered only the cobalt containing alloy might fit in this category.
- Dynamic Desorption Plateau Pressure - must be high enough to generate pressures above atmospheric pressure at moderate temperatures. Liberating the captured hydrogen with the use of low-grade waste heat from some other process is extremely attractive from the economic point-of-view. Hydrogen release can be considered an extreme bottoming cycle for any co or poly generation system (target Pd >2 atma at 80° C).

Initially five alloy compositions were considered for this application. Four of the candidate alloys were lanthanum-nickel with small addition of various other metals (Al, Co, Fe, Sn). The fifth alloy considered contained Ca, Ni and Al. See Figures 11-15.

Alloys I and II, the iron and tin substitutions, $\text{LaNi}_{3.8}\text{Fe}_{1.2}$ and $\text{LaNi}_{4.7}\text{Sn}_{0.3}$ respectively, were eliminated because of their sloping plateau and greatly reduced capacity, See Figures 11 and 12. Even though the plateaus were approximately at the correct pressure, demonstrated poor kinetics was also a contributing factor in this decision.

Alloy III ($\text{CaNi}_{4.9}\text{Al}_{0.1}$), although it had a flat plateau at the right pressure, its excessive hysteresis and low capacity caused it to be rejected., The undesirable hysteresis characteristic would require water temperature to be greater

than 80°C to raise the desorption plateau above the desired discharge pressure of 2 atmospheres absolute, see Figure 13.

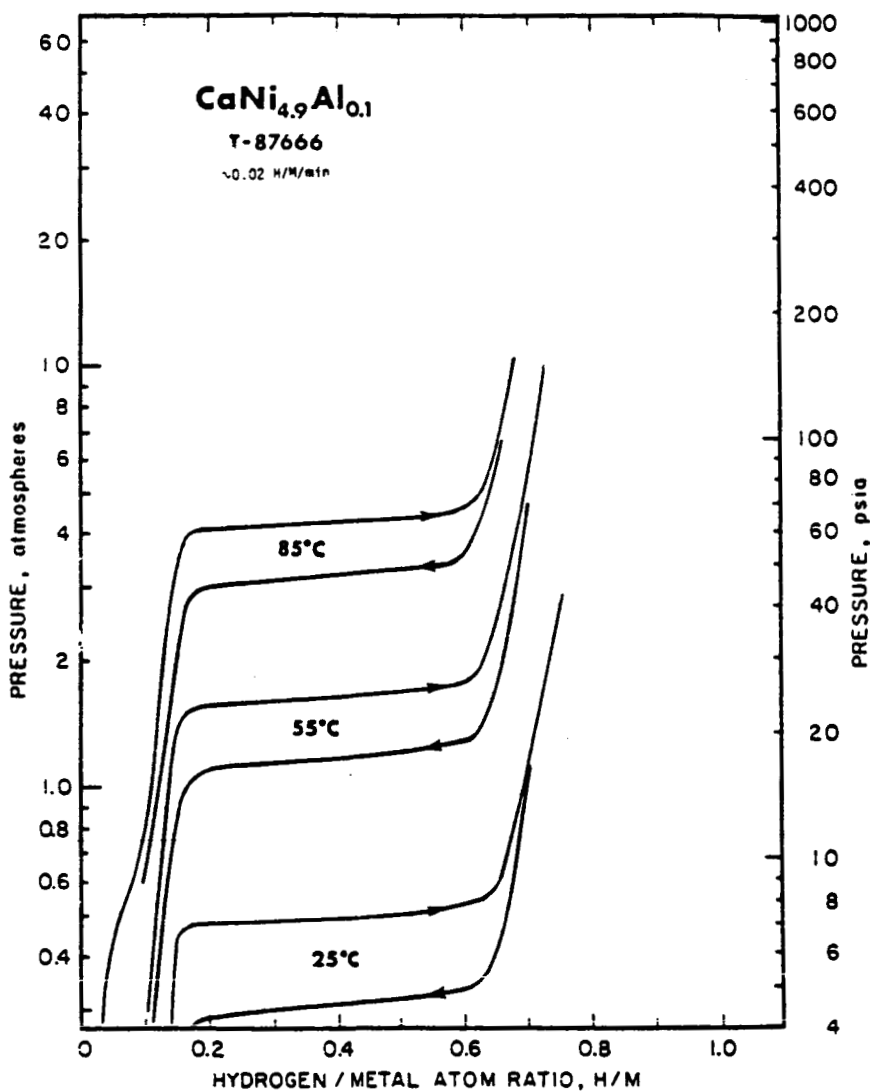


FIGURE 13: Dynamic pressure-composition isotherms for CaNi_{4.9}Al_{0.1}. Ref. 4.

Candidate alloy IV, (LaNi₃Co₂), or a slightly modified version of it, will probably work very well; but because it contained cobalt which might be a problem to obtain in large quantities, it too was eliminated. Figure 14 depicts its acceptable properties and Figures 4 and 8 show its moderately poor kinetics.

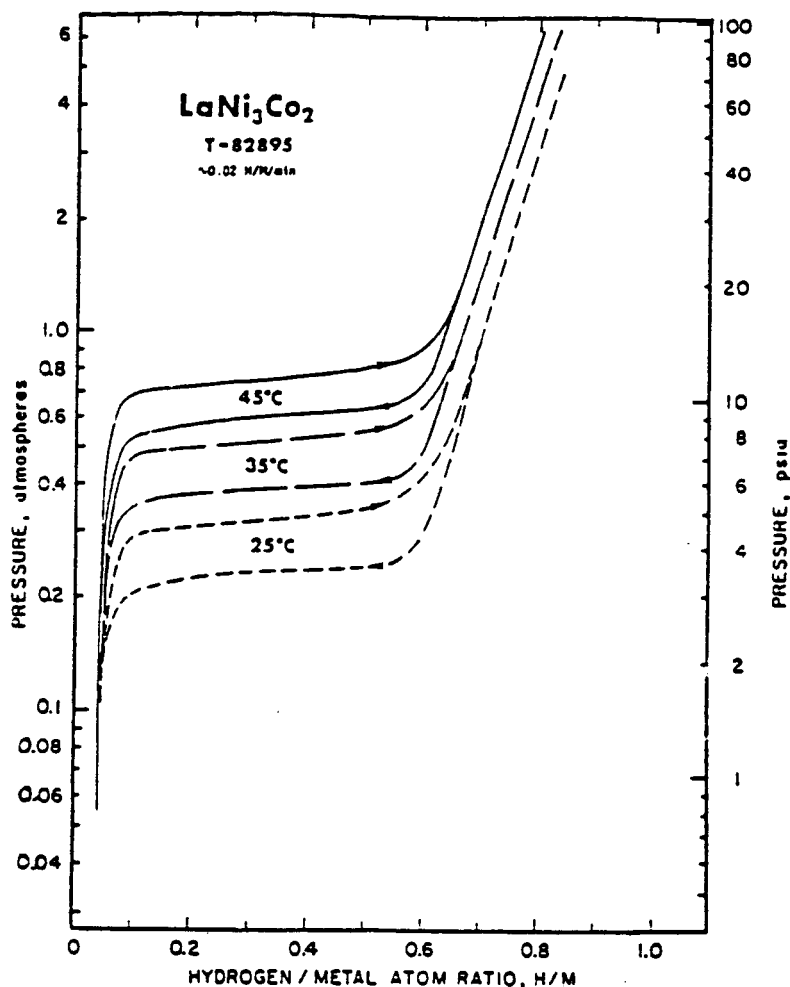


FIGURE 14: Dynamic pressure-composition isotherms for LaNi_3Co_2 . Ref. 4.

Alloy V ($\text{LaNi}_{4.7}\text{Al}_{0.3}$ -HYSTOR 207) closely approximated all the desired qualities except that the absorption plateau pressure was too high. By comparing Figures 15, 16, 17 the negative effect on the hydrogen storage capacity of aluminum substitutions for nickel is apparent. Greater additions of aluminum would have two major effects on the alloy developed; one desirable and one undesirable. The absorption plateau would be further depressed to the desired pressure but further reduction in hydrogen capacity would undoubtedly result. Because past work in this area had shown that the capacity loss would be small; and because the kinetics of this family of alloys is known to be extremely fast, we chose to melt a sixth alloy with an even higher aluminum content.

Alloy VI ($\text{LaNi}_{4.6}\text{Al}_{0.4}$ Heat T-88855-2) was melted and annealed (1125°C for 17 hours) and although the exact composition was not attained, the plateau depression can be seen by comparing Figures 15 and 18.

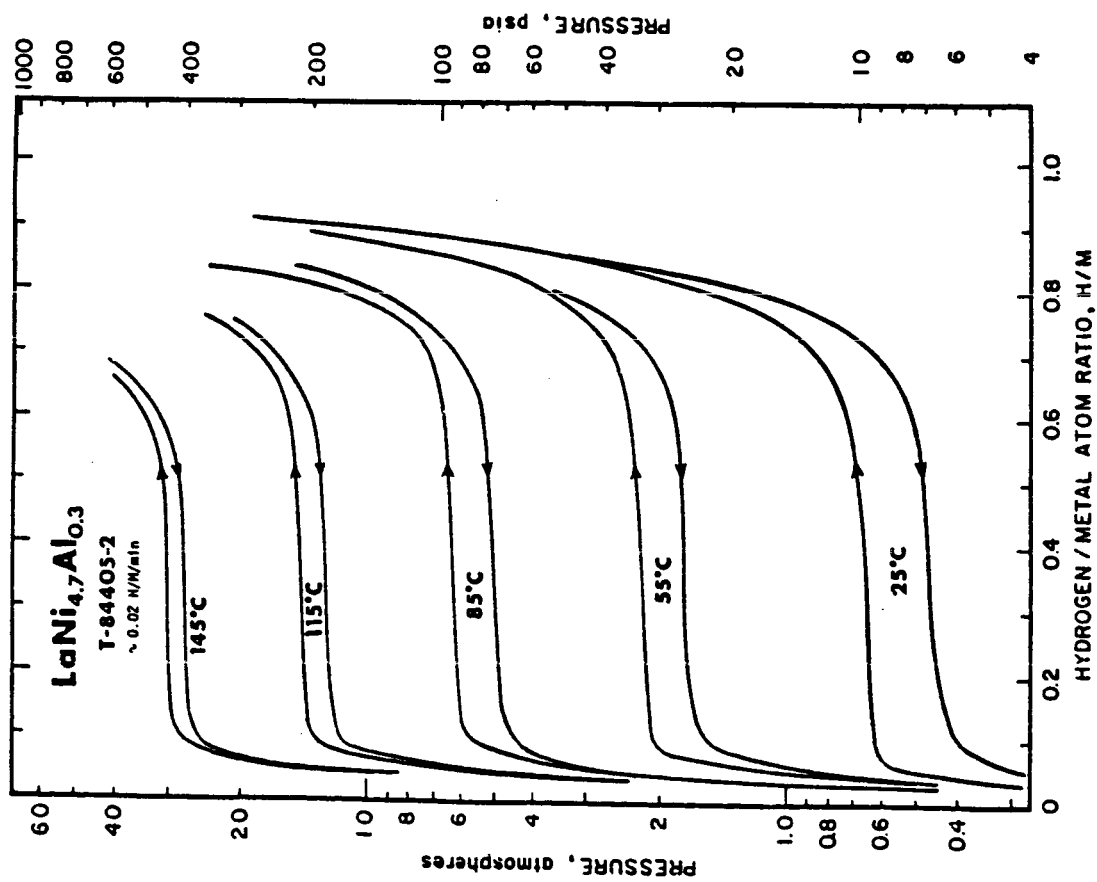


FIGURE 15: Dynamic pressure-composition isotherms for LaNi_{4.7}Al_{0.3}. Ref. 4.

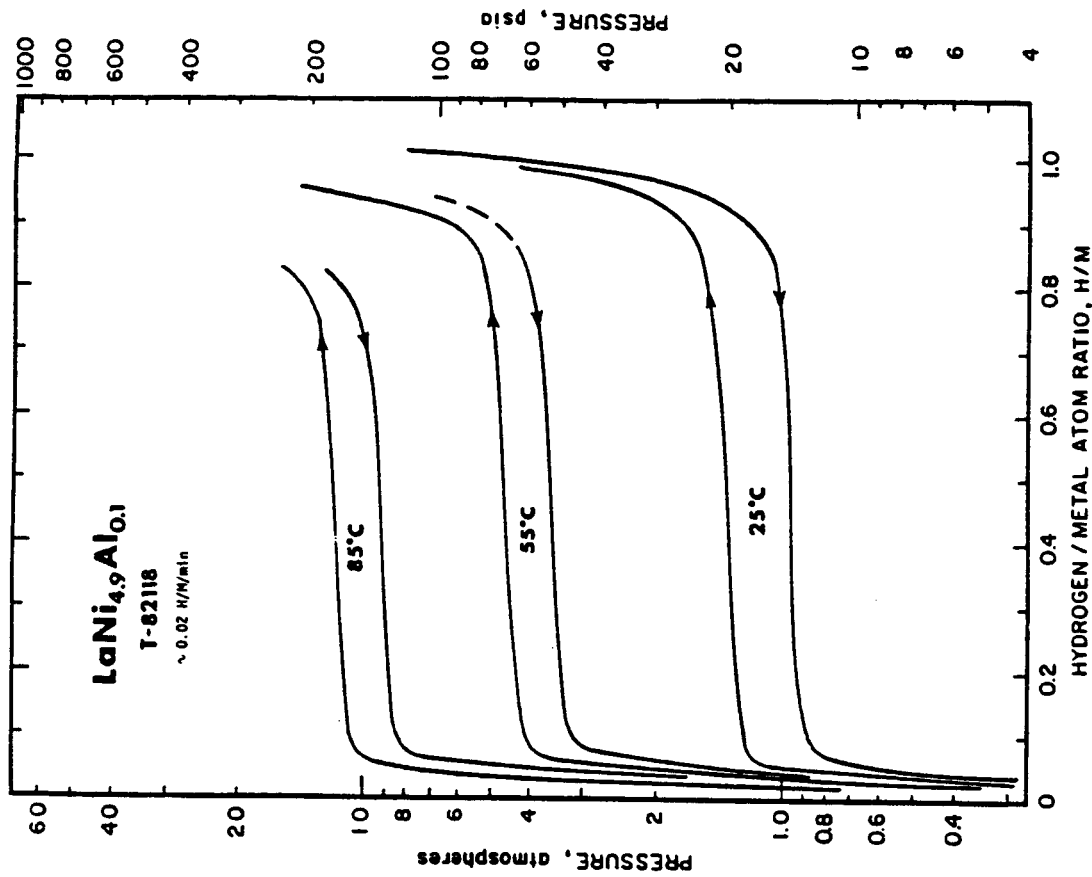


FIGURE 16: Dynamic pressure-composition isotherms for LaNi_{4.9}Al_{0.1}. Ref. 4.

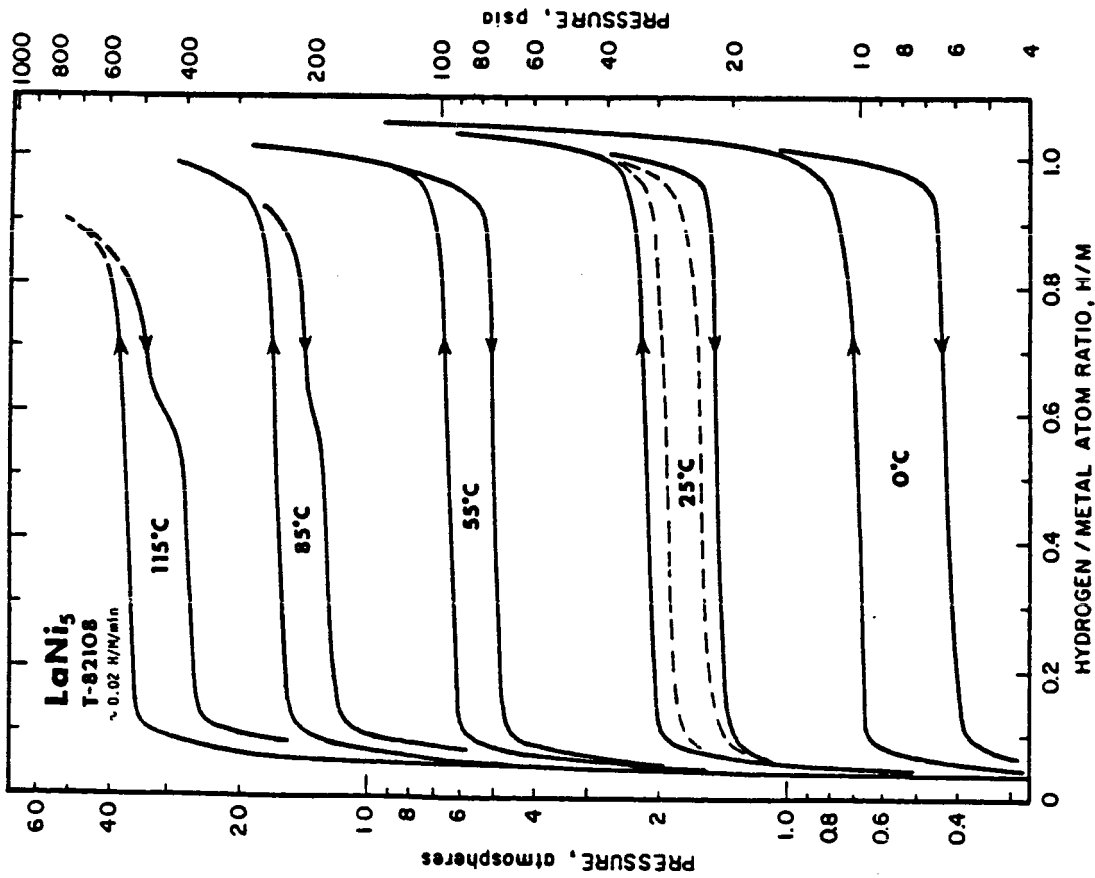


FIGURE 17: Dynamic pressure-composition isotherms for LaNi₅. For comparison the static isotherms are included at 25°C (dashed lines). Ref. 4.

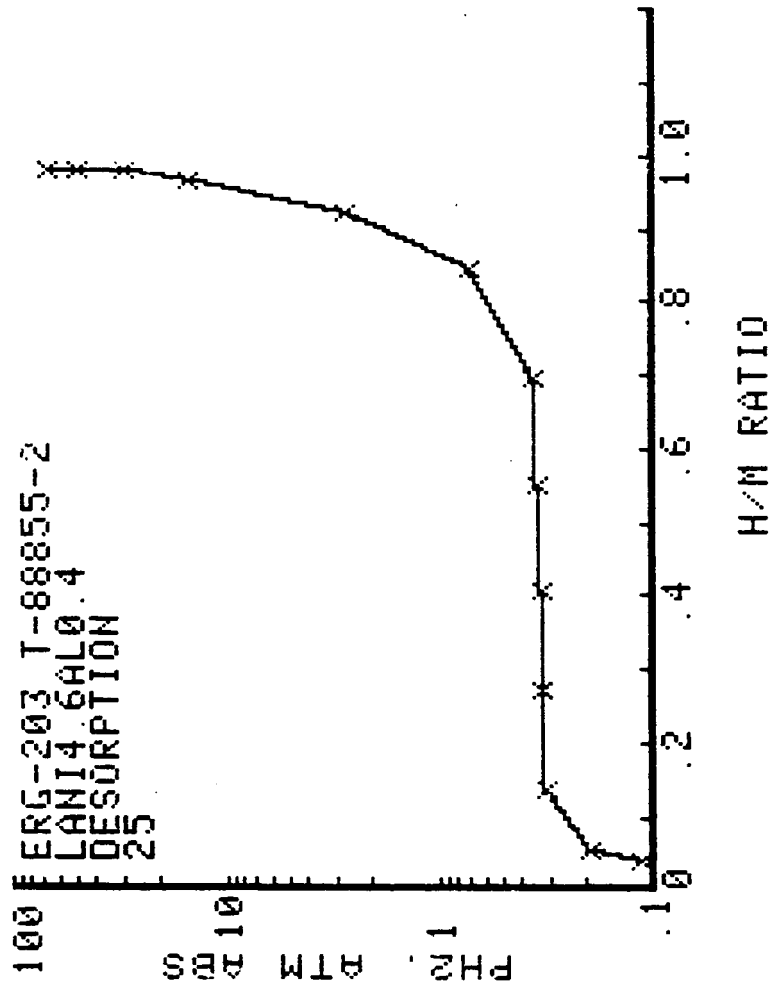


FIGURE 18: Isotherms of first experimental melt (actual composition LaNi_{4.68}Al_{0.32}) at 25°C.

When the natural log of pressure is plotted vs. reciprocal absolute temperature, for a fixed hydrogen concentration (usually mid-plateau), the result is linear and is referred to as a Van't Hoff plot. Figure 19 is a composite plot of a few of the alloys considered. LaNi₅ is also presented for reference purposes. It can be seen that Alloy VI can absorb H₂ at sub-atmospheric pressures at 25°C and can liberate the gas at pressures >1 atmosphere at 80°C. See Table 6 for the properties of the candidate alloys.

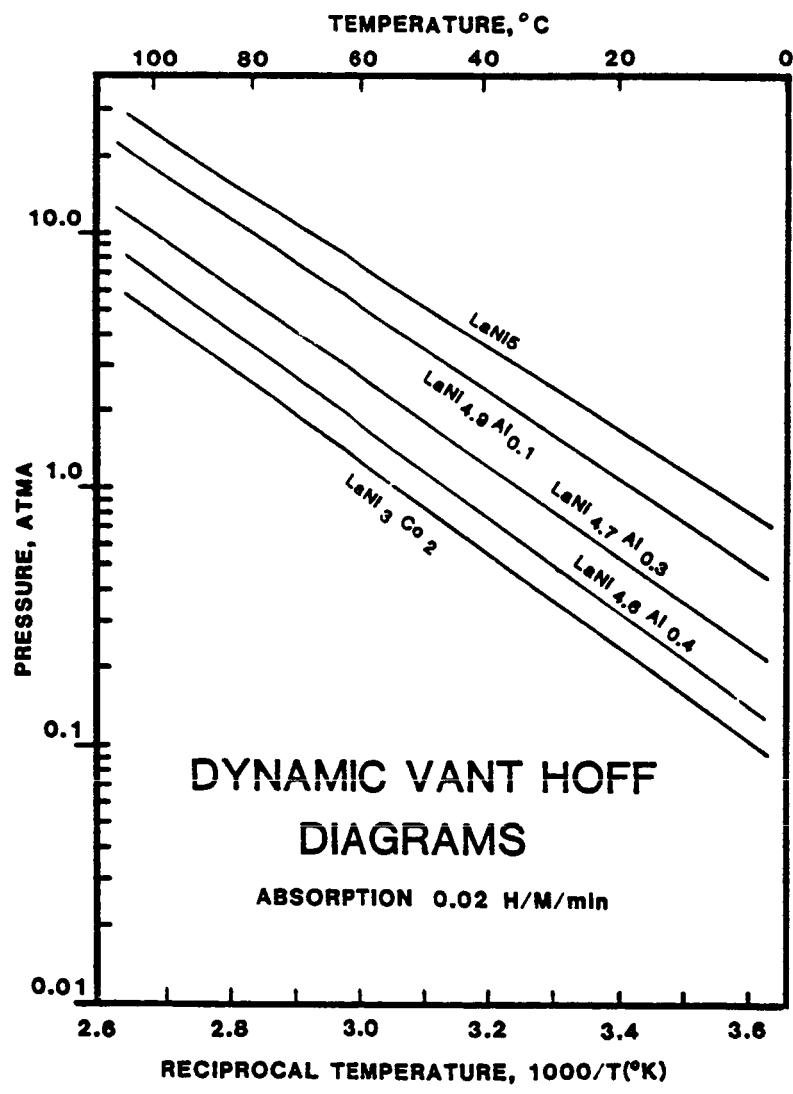


FIGURE 19: Van't Hoff diagrams for candidate alloys with LaNi₅, for reference.

Candidate Number	Alloy Composition	25°C Dynamic Absorption Pressure		Normalized Over Pressure ATMA	25°C Dynamic Hysteresis ATMA Pa - Pd	Temperature For 2 ATMA Discharge °C	Time to 50% Absorption Sec
		Pa	Pd				
		ATMA	Pd	ATMA	Pa - Pd	°C	Sec
CONTROLS							
	LaNi ₅	2.31	1.50	5.88	0.43	34	5.6
	LaNi _{4.9} Al _{0.1}	1.63	1.16	4.09	0.34	51	17
V	LaNi _{4.7} Al _{0.3}	0.65	0.47	1.63	0.32	60	25*
IV	LaNi ₃ Co ₂	0.35	0.24	0.88	0.38	80	92
I	LaNi _{3.8} Fe _{1.2}	0.82	0.52*	2.06	0.45**	76**	550
II	LaNi _{4.7} Sn _{0.3}	0.61	0.41	1.53	0.40	73**	80
III	CaNi _{4.9} Al _{0.1}	0.50	0.31	1.26	0.48	71	***
VI**	LaNi _{4.6} Al _{0.4}	0.40	0.30	1.00	0.29	72	25

* Estimate based on extrapolation of static data

** Estimate based on limited data

*** Not enough data available for estimate to be made

**** Hysteresis = $\ln(Pa/Pd)$ Where Pa = absorption pressure) Pd = desorption pressure) at plateau midpoint

Data for Alloys I - V and control alloys are taken from Reference 3.

TABLE 6: CANDIDATE ALLOY PROPERTIES

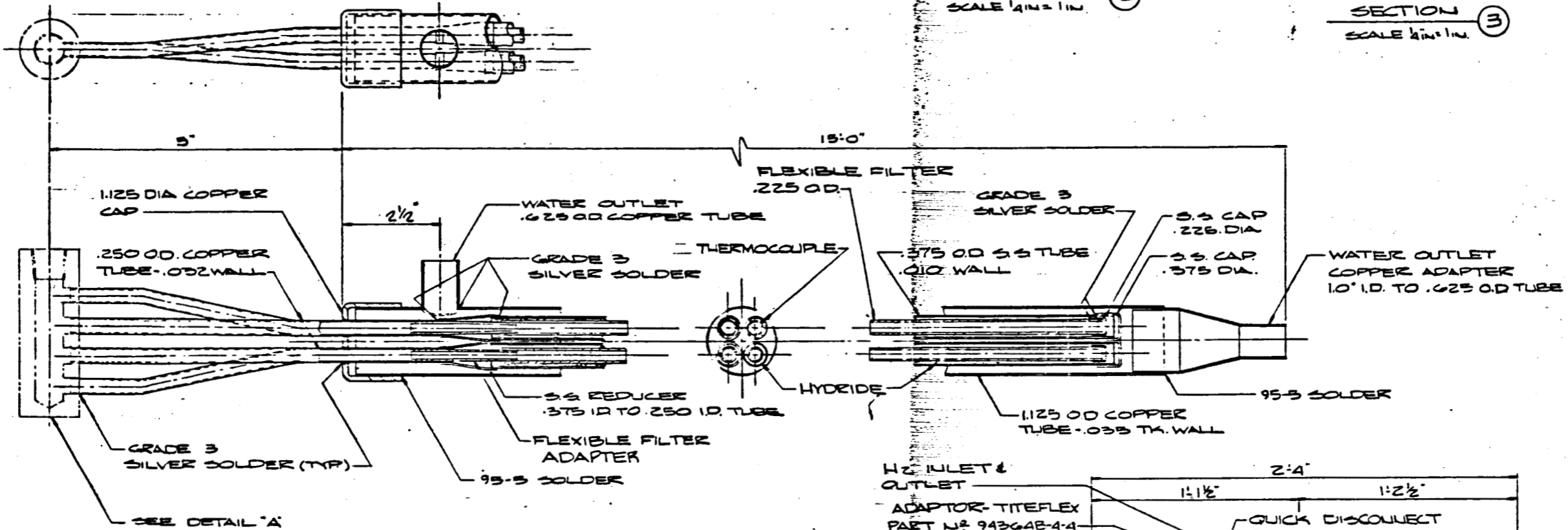
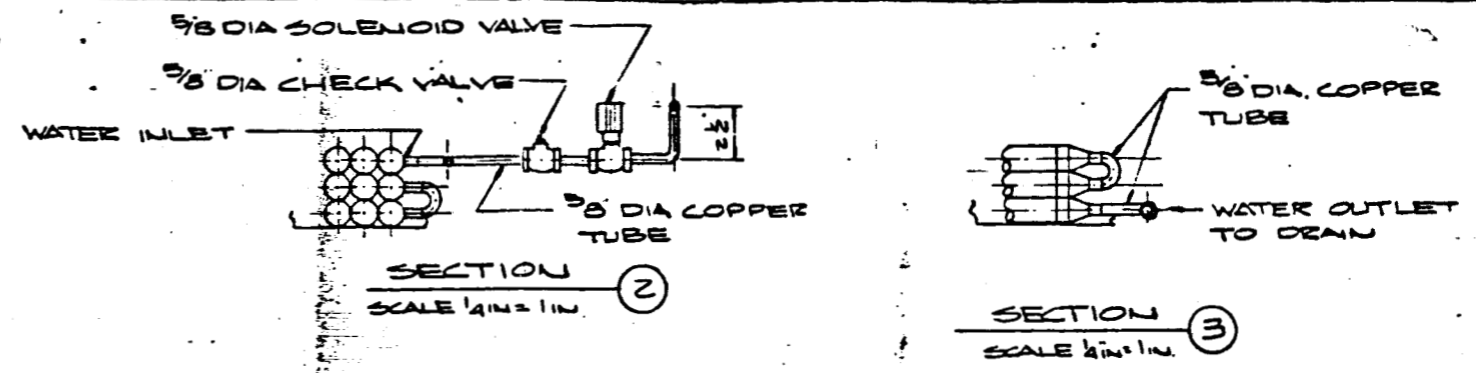
C. Task 3 - Hydride Container Design

The absorption of hydrogen by metal hydride is a highly exothermic reaction and conversely is endothermic upon desorption. The rate at which the hydrogen must be absorbed or desorbed determines the method of heat management used. Two approaches generally used in the design of hydride vessels is an isothermal design, where the heat of reaction is either removed or added by means of a heat exchanger with a thermal transport fluid and an adiabatic design where the heats of reaction are stored within the bed by the incorporation of large quantities of high heat capacity-inert materials. Since the heat transport paths are shorter in the adiabatic system, that approach is used for the higher hydrogen absorption/desorption rates. Where hydrogen flow-rates are low enough the isothermal process is used since smaller and fewer vessels are required with a greatly reduced hydride inventory leading to a desirable effect on the economics of the system.

Because of the encouraging results obtained during the performance of Task 1, a decision was made to use an isothermal design for the management of the generated heat. The rapid hydrogen flow-rate made it mandatory to keep the hydride "bed" thin thus reducing the length of the heat transfer path. During absorption, cooling water is made to flow around small diameter (.375 in. OD) tubes in which the hydride is contained. A flexible filter, of cylindrical cross section, is placed in the tube with the hydride occupying the annular space between the filter and the cylinder wall. Since the filter runs the full longitudinal length of the tube it provides a low pressure-drop path for the low pressure hydrogen vapor to enter the system.

The gas is very rapidly absorbed by the metal to which it is exposed and the heat of reaction dissipates through the outer wall into the cooling water. For details of construction see Figure 20. As shown on the same figure, four of the 25 ft. long 0.375 in. OD tubes are placed into a 1.125 in. OD water jacket, and spirally wound to a 27 in. diameter flat coil. Three coil assemblies were fashioned in this way, placed inside an enclosure and the water jackets connected in series. The hydrogen lines, each equipped with a filter, pressure relief valve and a manual shut-off valve were connected in parallel to a central manifold through which the

hydrogen enters and exits the system. The enclosure also housed two electrically operated solenoid valves to control the hot (for desorption) and cold (for absorption) water flow through the jacket. Two motor-operated rotary-valves provide a low-pressure path for the hydrogen to flow from the source to the "bed". A differential pressure transducer, located between the two rotary valves, enabled monitoring of the pressure in the coil, at the source or both. The transducer range, -10 psi to +10 psi, accurately transmitted the low pressures and small changes witnessed during the operation of the device. A thermocouple in the hydride, another in the water jacket and a third in the air enabled recording of hydride, water and ambient temperatures during a test run. A pressure transducer (0-600 psig) was installed on the high-pressure side of a regulator to track pressure changes in the hydrogen cylinder source as the hydrogen was absorbed by the hydride.



COIL DETAIL
SCALE: FULL SIZE
3 REQ'D
NOTE: TUBING SHOWN BEFORE BEING COILED

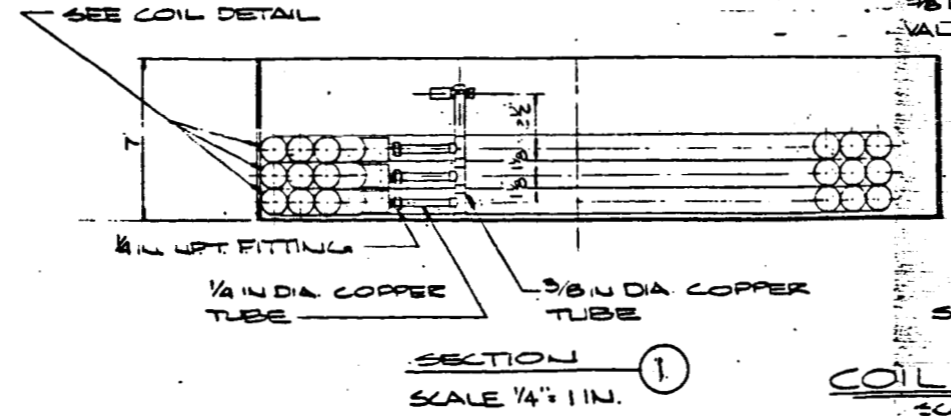
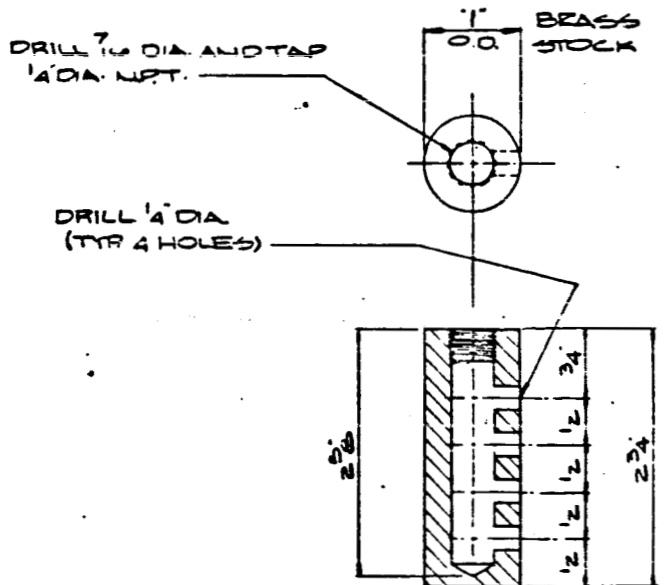
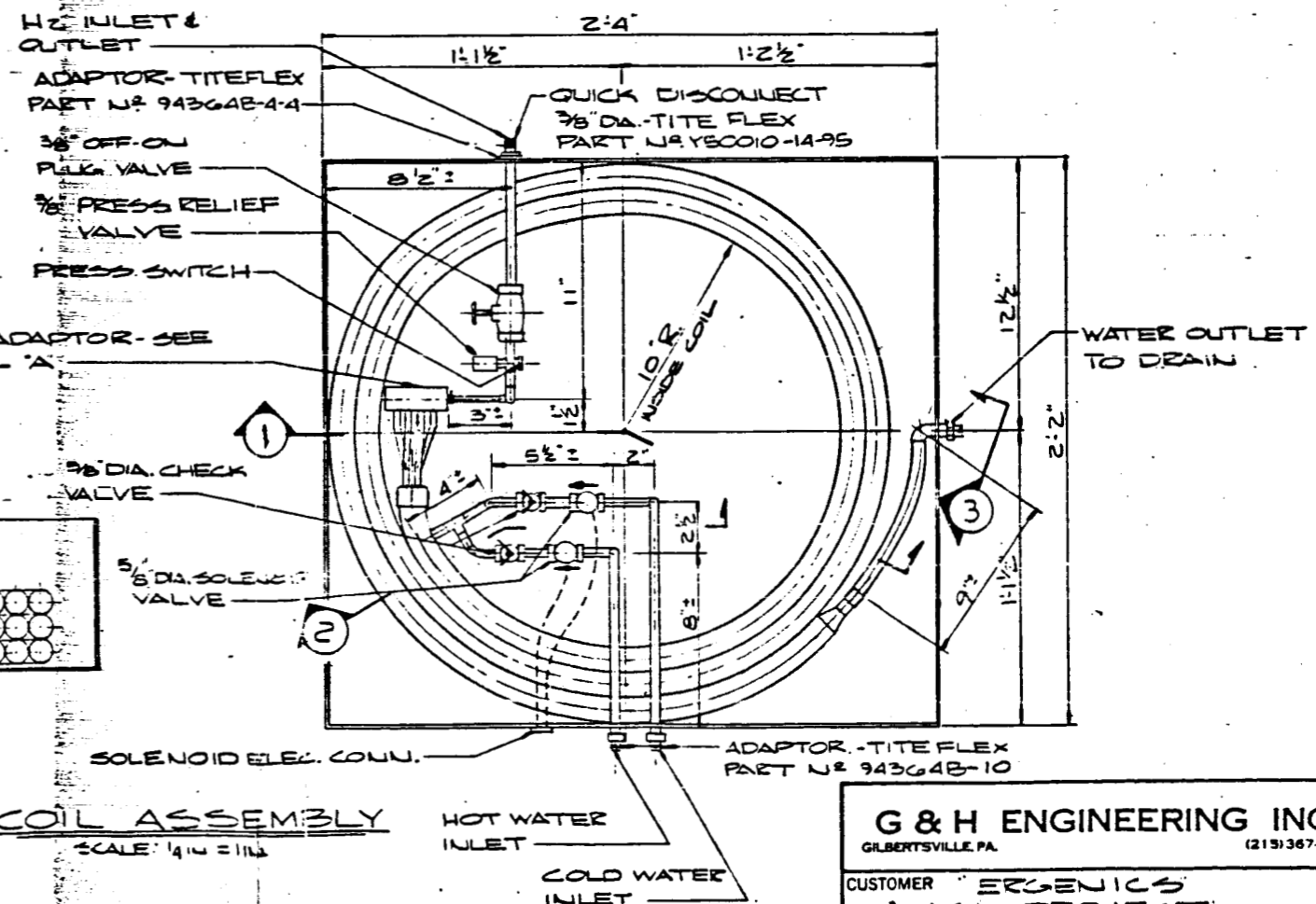


FIGURE 20

G & H ENGINEERING INC.
GILBERTSVILLE, PA. (219) 367-22

CUSTOMER: ERGENICS
NASA PROJECT

TITLE: HYDROGEN ABSORPTION COIL DETAILS

All temperatures and pressures as well as all electrical valve switches were monitored and operated remotely, from 50 feet away, for safety considerations.

D. Task 4 - Alloy/Container Design Verification Test

The design described in section C, i.e. 0.375 in. diameter copper tube with axial flexible filter and hydride filling the annular space between the two, had to be verified by flow tests. A single coil 10 ft. long was fabricated using 380 grams (38g/ft) of the specially melted alloy (LaNi_{4.6}Al_{0.4} heat T-88860-2) after grinding to -35 mesh. The hydride was vibrated into the tube/filter assembly's hydride space where the resulting void fraction is typically 40%. The tube was equipped with a pressure relief valve and a manual shut-off valve. The coil was not fitted with a water jacket; but was immersed in an agitated temperature-controlled bath instead. This provided better temperature control and nearly isothermal test conditions.

The verification test program emphasized the absorption half of the cycle since the rapid absorption of the low pressure hydrogen vapor was recognized as the constraining factor in this application. Hydrogen gas at various pressures slightly above and below atmospheric pressure was used to charge this coil while it was held at 25° C by the water bath. The time to reach 90% of full charge was recorded and the results are presented in Figure 21 and Table 7. At the system design pressure point (2 psig) the coil exhibited the capability to absorb 44 liters of hydrogen, 90% of the hydride's full capacity (1.16 wt%) within 2 minutes. This rate is 30 times faster than required for the subject application. The results of the tests verified the present heat exchanger design and suggested newer and less expensive approaches to hydride encapsulation.

Hydrogen Pressure psia	Time To 90%, Min	Abs. Rate Max, SLPM	Abs. Rate Avr, SLPM
7	>7.35	15.0	6.0
20	4.35	18.4	10.1
15	2.58	32.2	17.1
20	1.25	56.0	35.2
25	1.15	80.0	38.3
*17	2.0	40.0	22.0

* Interpolated values for dewar design pressure.

TABLE 7. Hydride Test Coil absorption rates at various charging pressures

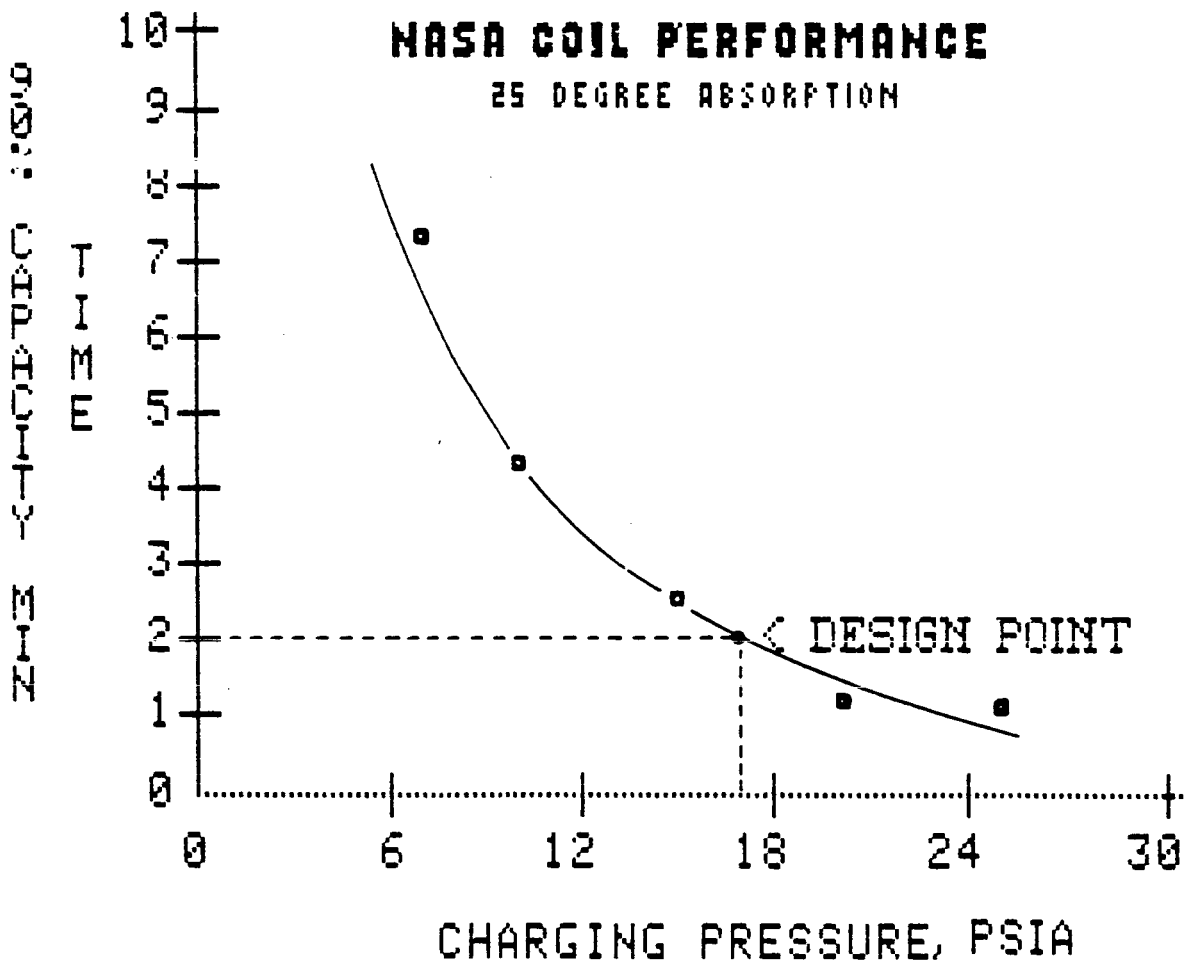


FIGURE 21: 25°C absorption rate performance of NASA test coil as a function of charging pressure.

E. Task 5 - Hydride Alloy Manufacture

Based upon the system design constraints and known hydride characteristics, a custom alloy of Lanthanum Nickel Aluminum was identified as the "hydride-of-choice". As described in Section B, Task 2, the hydride contained a higher aluminum content than Ergenics standard HYSTOR-207 (LaNi_{4.7}Al_{0.3}) alloy. A 30 lb melt was made in a vacuum induction furnace at the International Nickel Research and Development Center (IRDC) in Sterling Forest, NY. The melt was supervised by Dr. G. D. Sandrock of the Ergenics staff and the Chemical Analysis is presented in Table 8. The billet was normalized by heat treating at 1125°C for 17 hours and crushed in a Gyro Mill grinder to -35 mesh. A small representative sample (8.0 grams) was enclosed in a hydriding reactor and both absorption and desorption equilibrium isotherms were generated at three different temperatures. Figures 22-23 depict the measured Pressure-Composition-Temperature (PCT) characteristics of heat T-88860-2 melted for the application.

<u>Analysis Number</u>	<u>Date</u>	<u>Heat Number</u>	<u>Constituents, Weight Percent</u>					
			<u>LA</u>	<u>Ni</u>	<u>Al</u>	<u>O₂</u>	<u>N₂</u>	<u>C</u>
35631	8/12	T-88855						
		Target	33	65	2	.05	.01	.02
		Actual	33.2	65.1	1.7	.02	.01	
Atomic Formula - La _{1.02} Ni _{4.73} Al _{0.2}								
35713	8/16	T-88860						
		Target	33.1	64.3	2.6	.02	.01	.02
		Actual	32.9	65.0	2.1	.01	.002	
Atomic Formula - La _{1.00} Ni _{4.67} Al _{0.33}								

Table 8: Chemical Analysis Report

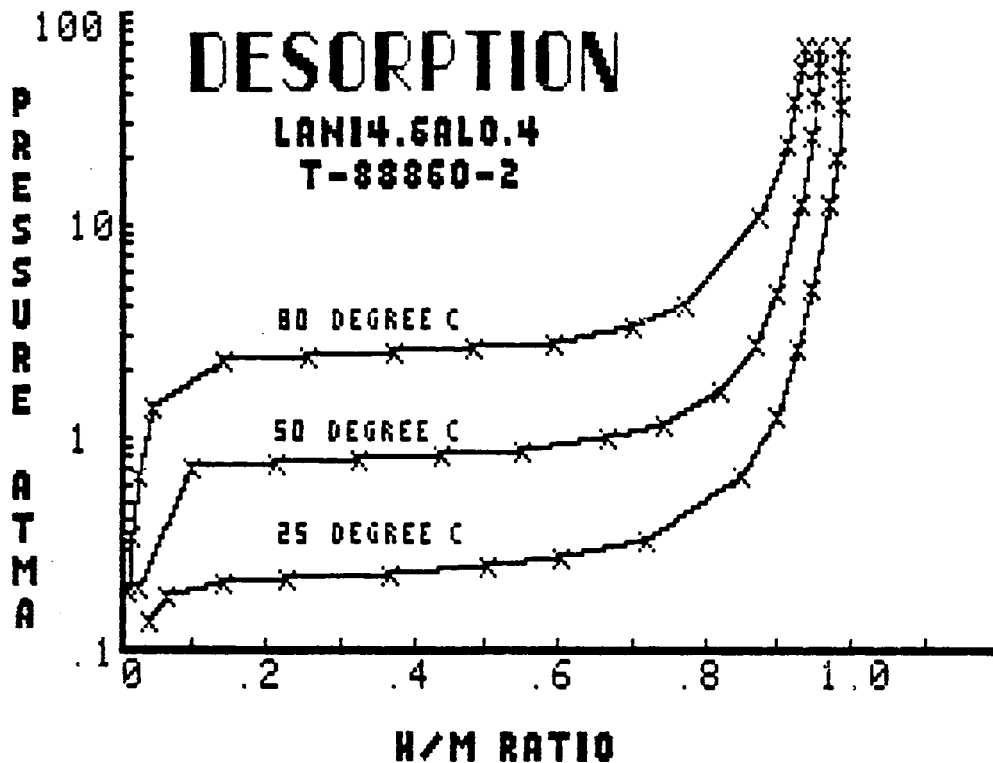


FIGURE 22: 25, 50 and 80°C desorption isotherms for LaNi_{4.6}Al_{0.4}, heat #T-88860-2

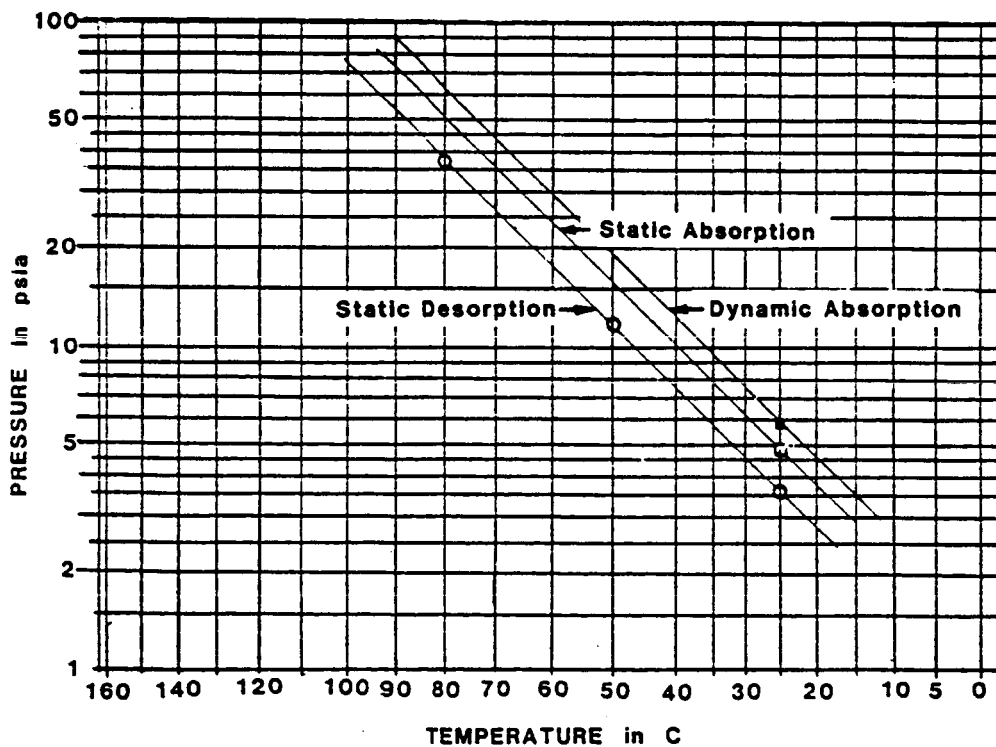


FIGURE 23: Equilibrium (Static) and Transient (Dynamic) 25°C Absorption and Desorption Van't Hoff curves for LaNi_{4.6}Al_{0.4} T-88860-2

An earlier melt, heat T-88855-2, did not meet composition or performance specifications. See Table 8 and Figure 18. Figure 22 shows the Pressure-Temperature relationship with the hydrogen concentration held constant at the isotherm plateau mid-point ($H/M = 0.5$). The dynamic absorption and desorption lines indicate that 25°C, 1.0 atma absorption and 75°C, 3.0 atma desorption is possible with this hydride.

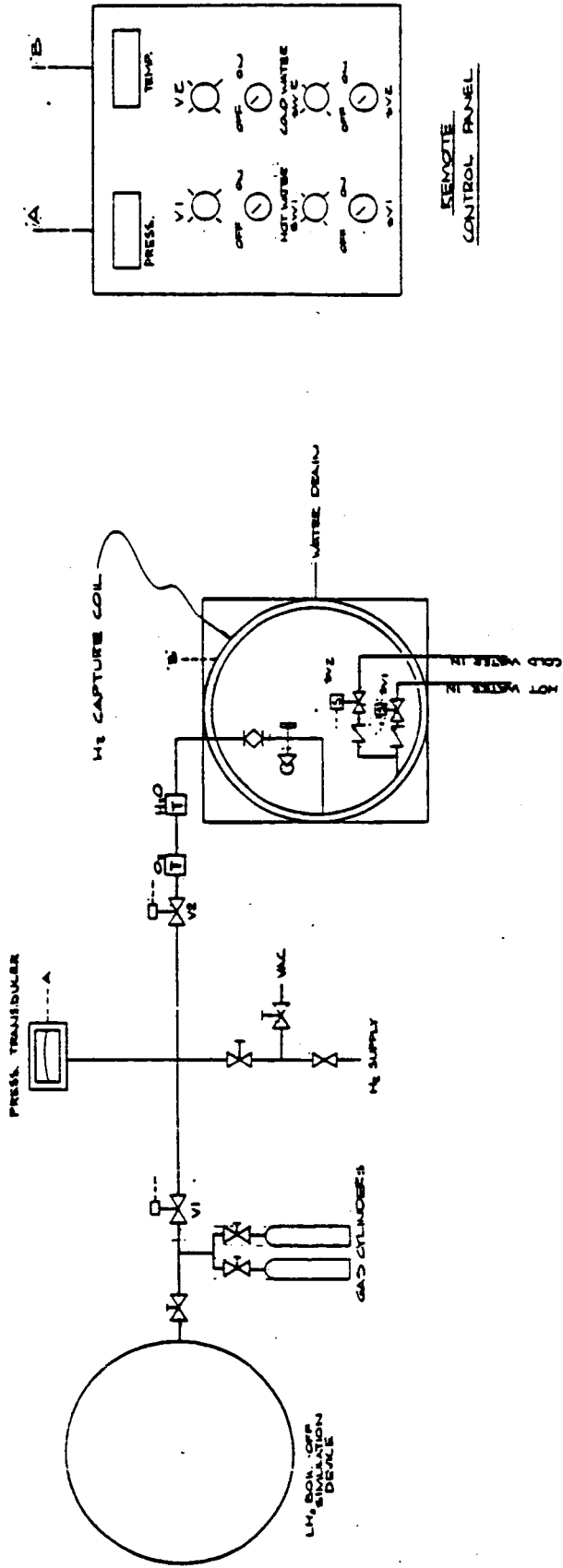
F. Task 6 - Container Construction and System Assembly

The system design, as described in section C, is based on coiled hydride tubes in a water jacket, See Figure 20. Twelve 25 ft. long, 3/8 inch diameter copper tubes were each fitted with a 0.225 inch diameter hollow flexible filter. The tubes with full length filters, were attached to a vibrator and positioned to stand on end. The annular space between the filter and the inner tube wall was filled with -35 mesh hydride powder to a packing density of 60%. Four tubes were inserted into each of three 1-1/8 inch diameter copper water jackets and soldered in place. The water jackets, with internal hydride tubes, were coiled into a flat spiral layer of approximately three wraps.

The hydride tube ends were fitted with individual 2 μ m filters and connected in parallel to a central manifold through which the hydrogen both enters and exits the hydride beds. Each coil layer was equipped with a 150 psi pressure relief valve and a manual shut-off valve. The three layered coils were stacked and bound together with their hydrogen manifolds connected in parallel, thus insuring free access by the entering gas to all the hydride beds simultaneously. This configuration provides the lowest possible pressure drop loss. The coil stack was placed into a steel-box-housing (30"x36"x16") and the water jackets connected in series. Series connection of the water lines results in greater sensible heat recovery and higher efficiencies. This method of cooling and heating was chosen even though more rapid absorption can be obtained by connecting the water jackets in parallel. Two thermocouples were placed in the coils; one in the hydride bed and one in the water jacket. The thermocouples would be used during the test program to monitor temperature transients as hydrogen is admitted or discharged from the coil and as water temperatures are changed. A third thermocouple was placed in the housing to monitor ambient temperature. Two motorized rotary valves were used to direct the

hydrogen flow from the low pressure source to the coil during absorption and from the coil to the low pressure gas accumulator during the discharge phase of the test (V-1 and V-2 in Figure 24). The hydrogen line was also fitted with an oxygen purifier and a molecular sieve dryer to protect the hydride surface from poisoning by the inadvertant admission of air during the performance of the test.

A low pressure differential pressure transducer (-10 psi to +10 psi) is located at a "tee" junction between V-1 and V-2, thus enabling very accurate pressure measurements of the hydride coil, the hydrogen source and during absorption, both. A pressure transducer was also installed on the high pressure side of the regulated hydrogen supply to monitor changes in the cylinder pressure as the hydrogen is absorbed by the hydride. From these measurements of gas volume absorbed as a function of time, absorption rates can be calculated. Two solenoid valves (SV-1 and SV-2 in Figure 24) control the hot and cold water to the coil water jackets. External to the housing, manual shut-off valves are provided for evacuating and purging the system during set-up as well as for choosing the preferred hydrogen supply for each test. The motorized and solenoid valves are operated remotely (50 feet) by toggle switches mounted on the face of the control panel. Temperatures and pressures are monitored from digital readout instruments which are also mounted on the panel face. See Figures 25 and 26 for photographs of capture device and remote control panel.



G & H ENGINEERING INC.	
CUSTOMER: ERLENJICS	
NASA PROJECT	
TITLE: DEMONSTRATION SCHEMATIC	
DATE: 10/18/81	ISSUE: NO
DES: Z	APP: 10/18/81
REVISION: 783-07 DZ 1	

NO	BY	DATE	REVISION

FIGURE 24: Schematic of capture vessel test set-up at KSC.

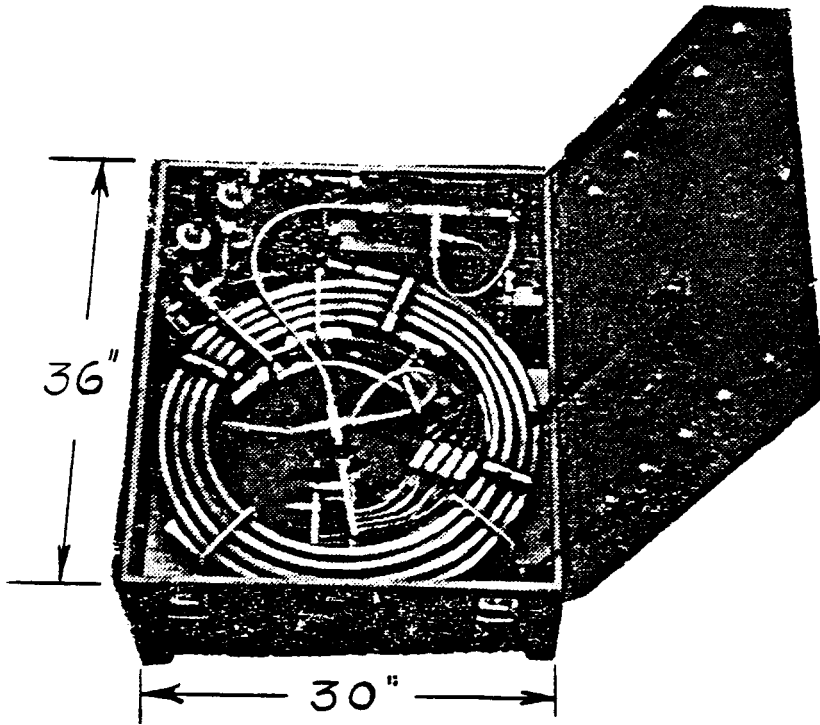


FIGURE 25: Hydrogen boiloff capture system.

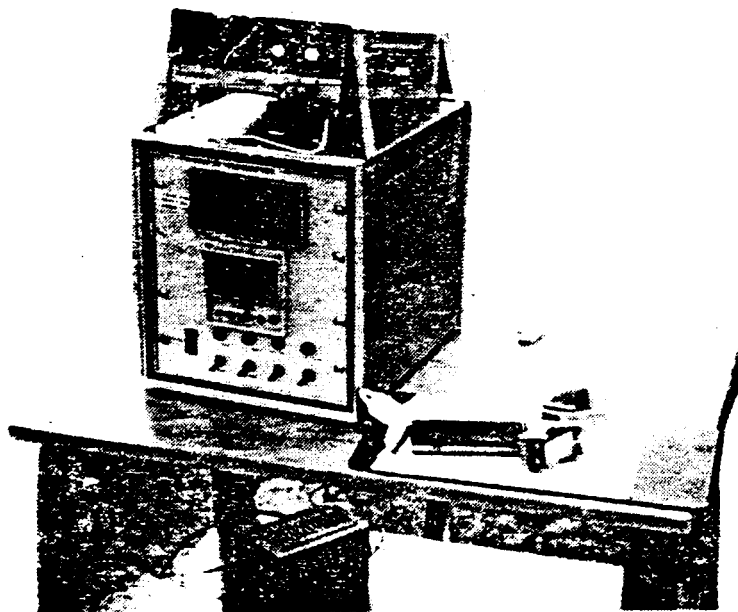


FIGURE 26: Remote control panel for KSC demonstration.

G. Task 7 - System Test

The test of the demonstration device was conducted in two parts. The first, Task 7, involved testing under controlled conditions at the Erganics, Inc. laboratory in Wyckoff, NJ and the second, Task 9, was conducted "in-the-field", under less controlled conditions, at the Kennedy Space Center.

To simulate the low-pressure high-flow-rate hydrogen boiloff stream it was decided to use large balloons as the hydrogen source. This seemed, at first, to be a very simple and more-than-adequate solution since a balloon's internal pressure is extremely low (measured to be 0.01 to 0.05 psig) and essentially constant for the entire deflation period. Hydrogen absorption rate by the hydride is graphic and can be recorded as the balloon's diameter, hence its volume, is measured periodically during the run. A problem arose as this scheme was attempted with the small test coil as a result of a) residual air in the balloon due to insufficient purging, b) oxygen and/or water vapor permeation through the skin of the balloon or c) leached from the balloon material by the hydrogen. Whatever the reason, the effect was to poison the hydride's surface and reduce its storage capacity and chemical kinetics. The hydride was readily restored to its full capacity by evacuation to 1 mm Hg at 80°C and exposure to UHP hydrogen. Three different balloon materials were tried with various levels of success. See Figure 27. In the "as-received" condition none of the materials were acceptable. Washing with freon and acetone seemed to improve their performance; but the best results were obtained by coating the inside of natural-rubber advertising balloons with silicone vacuum grease. Using this procedure an eight foot diameter natural-rubber balloon was prepared for the demonstration at the KSC with the large coil system.

10 ft NASA COIL BALLOON ABSORPTION TEST

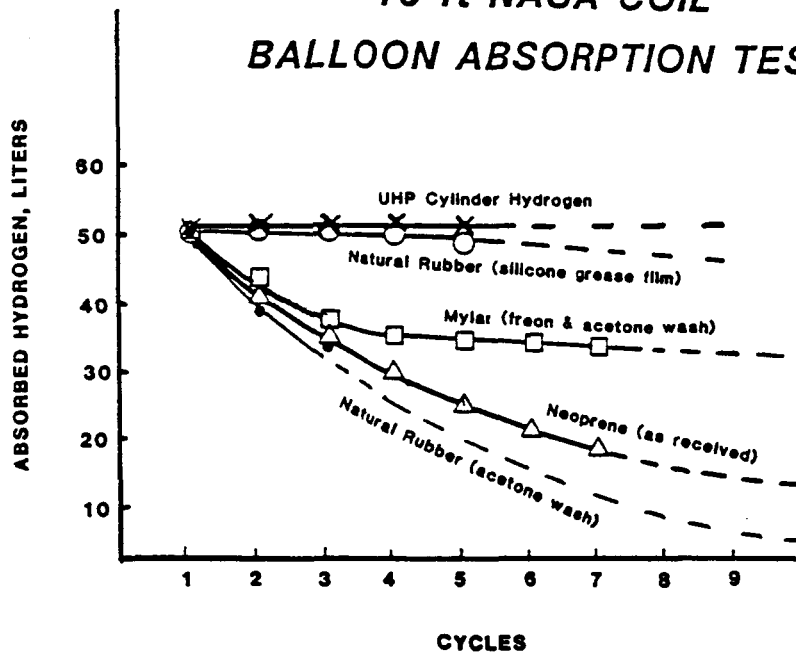


FIGURE 27 Effect of hydrogen stored in various elastomers on cyclic absorption capacity of hydride.

The laboratory absorption tests were conducted using a compressed gas cylinder as the hydrogen source and low-pressure regulation to reduce the pressure to atmospheric. The cooling water temperature was unregulated at an average temperature of 12°C and was circulated through the water jacket at a flow-rate of 6 GPM. With valve V-1 closed and V-2 open, the coil (hydride plateau) was measured at the pressure transducer as 3 psia (0.2 atma). The hydrogen absorption rate was measured by recording the cylinder pressure as a function of time. Ideally, as shortly as possible after opening V-1 the system pressure should have risen to near atmospheric pressure, which would most closely simulate the anticipated conditions during boiloff recovery at the KSC. This did not happen since the hydride's ability to absorb hydrogen, even at the sub-atmospheric charging pressures (10 psia, 0.7 atma) was much greater than the regulator's ability to dispense hydrogen. The result of this test is depicted as the solid dots (Small C_v Regulator on Figure 28. A second run with the same test conditions, but using a regulator with a larger C_v , resulted in the curve described by the open dots (Large C_v Regulator) also in Figure 28. Even in this run, although much improvement is evident, the coil was still "starved" by the regulator's inability to output hydrogen at a rate rapid enough to

satisfy the coil. Desorption of the coil after each run under controlled conditions confirmed that the maximum storage capacity, 68 SCF, of hydrogen had been absorbed in less than 10 minutes and that 90%, 60 SCF, had been absorbed in less than 3 minutes. A third test was run after returning from the KSC demonstration to confirm that the storage capacity and kinetics are unaffected after poisoning and subsequent reclamation. Using a bank of gas cylinders as a low-pressure (14.7 psia, 1 atma) surge and "feeding" the surge through a very large C_v regulator it was possible to run the test under conditions that more closely simulated the boiloff capture conditions during off-loading. The results are presented in Figure 28 as the open square points. The rapid initial rise, 50% absorbed in less than 1.5 minutes, is somewhat balanced by a slowing down above 80%. We attribute this to heat transfer limitations; but it should be recognized that the hydride need only reach 90% in less than 60 minutes to capture the off-loading boiloff.

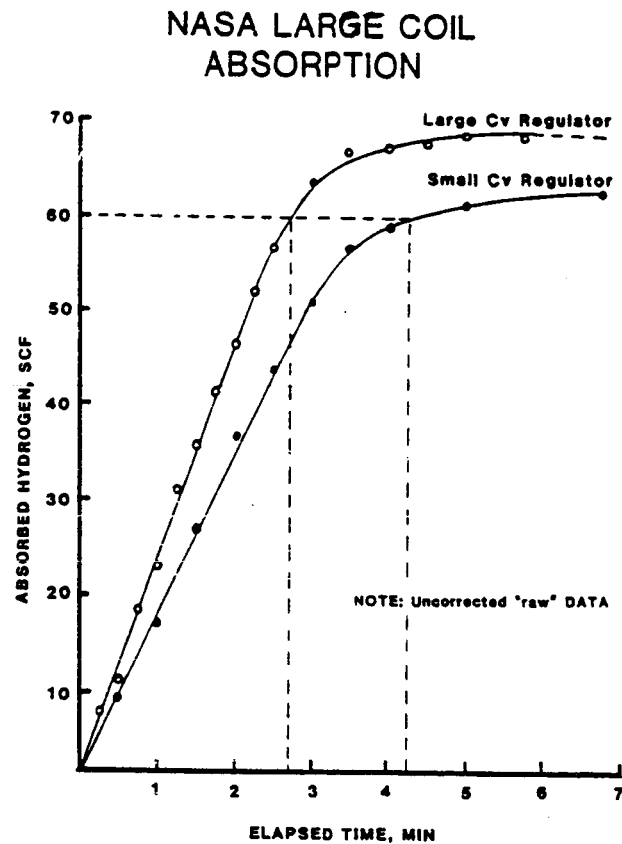


FIGURE 28: NASA hydrogen capture demonstration system performance.

H. Task 8 - Report Preparation

The preparation of the final report was an on-going effort with sections, figures and tables being prepared as required for monthly Progress Letter reporting. At the conclusion of the test program approximately 15% of the final report had been completed.

I. Task 9 - Proof of Concept Demonstration and Project Review

The device was operated at the KSC for evaluation by the Project Manager and other interested NASA and EG&G personnel.

Because of the uncertainties that still existed concerning the balloon poisoning effect, the field test procedure was planned to first demonstrate the absorption of pure hydrogen from a compressed gas cylinder, the second was to inflate the balloon with the hydrogen liberated by the hydride as hot water was circulated through the water jacket, and finally an attempt would be made to re-absorb the hydrogen from the balloon into the hydride.

The two regulators used at Ergenics for the first two absorption tests were piped in parallel so that the contribution of each might be enough to adequately "feed" the coil. Because of a water main break, cooling water had to be pumped from a water tanker. The cooling water was warmer (19-20°C) than optimum and once again the hydrogen flow-rate through the regulators was insufficient to supply the hydrogen at the hydride's absorption rate. The system pressure stayed below 0.5 atma for 2.5 minutes and rose to 0.8 atma when the regulator setting was increased to >40 psig. The total time to 90% capacity when the system pressure finally reached 1.0 atma was 8.0 minutes; much longer than the laboratory results but still very acceptable.

The liberation of the hydrogen from the hydride bed into the balloon was attempted. With V-1 closed and V-2 opened SV-2 was closed and SV-1 opened. This permitted hot water (73°C) to flow through the water jackets, raising the hydride temperature and thus increasing the system pressure. In about 1.0 minute, when the system pressure was above 2.0 atma, V-2 was opened to permit the hydrogen to

inflate the balloon. The balloon inflated rapidly, accepting approximately 70% of the hydrogen stored in the hydride within 5 minutes. Due to windy conditions, it was decided to abort and begin the third test quickly. The positions of SV-1 and SV-2 were reversed causing cold water to flow through the water jackets. With both V-1 and V-2 open, the balloon's diameter began to decrease as the hydrogen was reabsorbed into the bed. Due to a number of problems only half the balloon's volume was absorbed into the bed. The hydride had been damaged as a result of poisoning by oxygen, water vapor or some other substance emitted by the balloon's material. The apparatus was returned to the Ergenics Laboratory where the hydride was regenerated and additional tests run. The tests confirmed that hydrides can absorb low-pressure hydrogen at a rate that is adequate to capture LH₂ boiloff during the off-loading operation and liberate the hydrogen at pressures greater than atmospheric using hot water at reasonable temperatures.

A presentation, including slides of the figures and tables in this report, was made describing the fabrication and test program. Copies of all presentation materials and computer programs used during the performance of this program will be delivered to NASA/KSC with this report.

IV FULL SCALE SYSTEM

During the off-loading operation, hydrogen vapor is liberated at an average rate of 10,300 SCFM. A liquefier capable of producing 40 tons/day of liquid would be required to handle this off-gas in "real-time". Obviously, this is not a cost-effective approach. Even though a full-scale metal hydride boiloff capture system will require miles of tubing and many pounds of hydride, this work indicates that it is a feasible and economically justifiable approach to reducing launch costs at the KSC. See Tables 1-3, 5.

The system must be capable of capturing and storage, albeit short-term, 3,400 lbs. (620,000 SCF) of hydrogen for subsequent liberation to a small, approximately 2 tons/day, liquefier. Some combination of a smaller hydride capture system operating in parallel with the 12 ton/day liquefier presently being considered by NASA might be an even more cost-effective approach.

Generally, the system outline in Table 2 is representative of what a reasonable system would look like. For all computer runs we assumed 1-1/8 inch OD copper tubing with 0.05 inch wall. The space between each spirally wrapped coil was held at 0.5 inches as was the vertical space between the stacked coil layers. The axial filter was held to be 0.225 inches with a hydride packing density of 60% in the annular space between the filter and the copper tube wall. The hydride's bulk density was assumed to be 420 lb/ft³ which is a good approximation for the alloy to be used. The minimum diameter for the smallest coil wrap was held constant at 2 feet. Only the coil layer's large diameter, the allowable stack height and the hydride's storage capacity were allowed to vary. The computer program allows changing any of the physical dimensions or constraints, and a program disc is included with this report which allows NASA personnel to investigate the system's sensitivity to parameter changes.

A typical system of this design would require 290,000 lbs. of hydride housed in 200,000 feet of tubing. With coil diameters and stack heights limited to 10 feet, we need 5 stacks of coils, each in its own cooling water vessel. The rough approximation of the hydride and the system cost was based solely upon the assumed storage capacity (e.g. 1%, 1.2% or 1.4%) and the total hydrogen stored, 3,400 lbs. The system cost was assumed to be 1.4 times the hydride cost (\$20/kg, \$9/lb). For the computer run presented in Table 2, the hydride's storage capacity was assumed to be 1.2%; and the resulting costs of \$2.6M for hydride, \$3.6M for the total system and a payback time of 2 years are projected. The payback time is based on 20 launches/year and is computed as follows. It does not include the liquefier initial cost, operating costs or interest on capital outlay.

20 launches x 9 off-loadings/launch x 6000 gal/off-loading = 1.08 x 10⁶ gal/year
400 gal/day normal boiloff x 360 days = 144,000 gal/year
Total boiloff reclaimed 1.22 x 10⁶ gal/year or \$1.84M/year at \$1.50/gal

The capture system can be integrated into the existing facility at LC-39 as pictured in Figure 29. The reliquefier, being small, can be located at the storage dewar top where its discharge can be added directly to the existing liquid. Multiple

capture vessel modules with appropriate valving will permit discharging of some while others may still be absorbing boiloff. Additional modules may be added as needed.

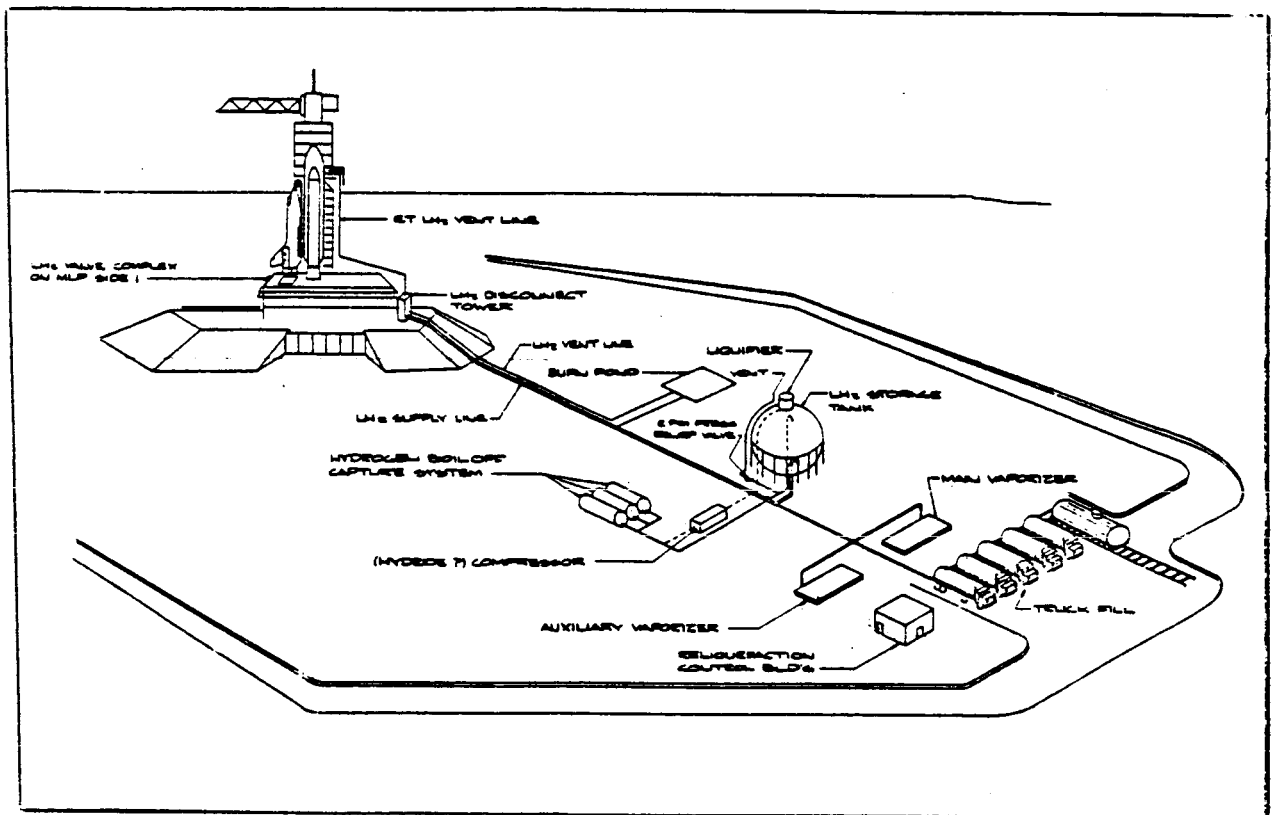


FIGURE 29: Artists concept of hydrogen boiloff recovery system at LC-39. Ref. 5.

Figure 30 shows schematically how the capture vessel, pictured in the upper right-hand corner, can be incorporated into the present system with a minimum of interruption and no change in present operating procedure. During installation the existing 10 inch - 150 lb. manual valve in the vent line would be temporarily closed, and the flanges broken, see Figures 31 and 32. The spool piece between the manual valve and the 10 inch - 150 lb. 2.5 psi check valve will be replaced by a flanged tee with the branch leading to another 10 inch - 150 lb. manual valve. At this point the existing manual valve can be reopened since all additional construction can take place downstream of the new 10 inch manual valve. The location of the check valve insures that the dewar cannot be subjected to excessive back pressure. Should the capture vessels not be able to absorb the boiloff vapor for some reason, the back pressure will unseat the check valve, venting the vapor as is presently done.

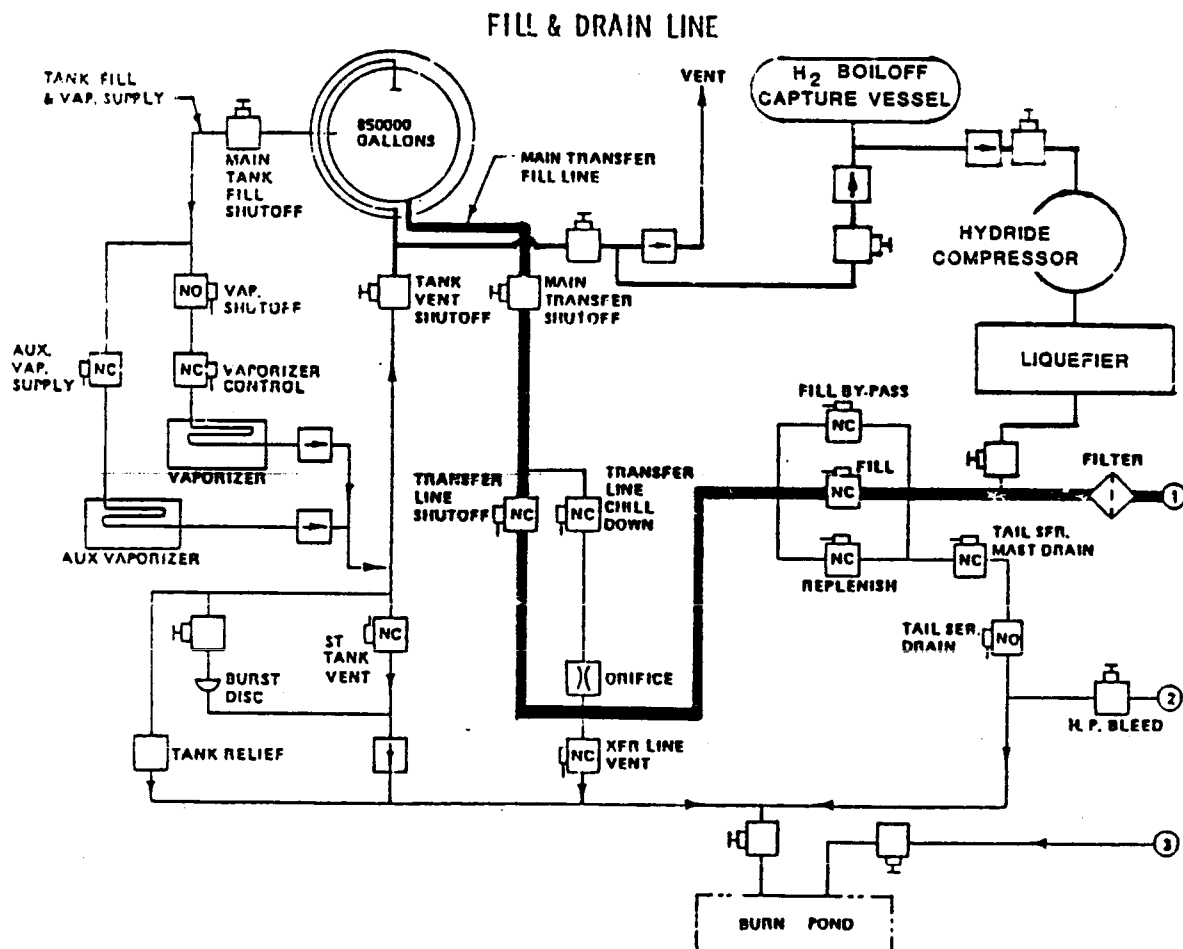


FIGURE 30: Schematic of hydrogen vapor recovery system addition to existing LH₂ fill and drain lines. Ref. 1.

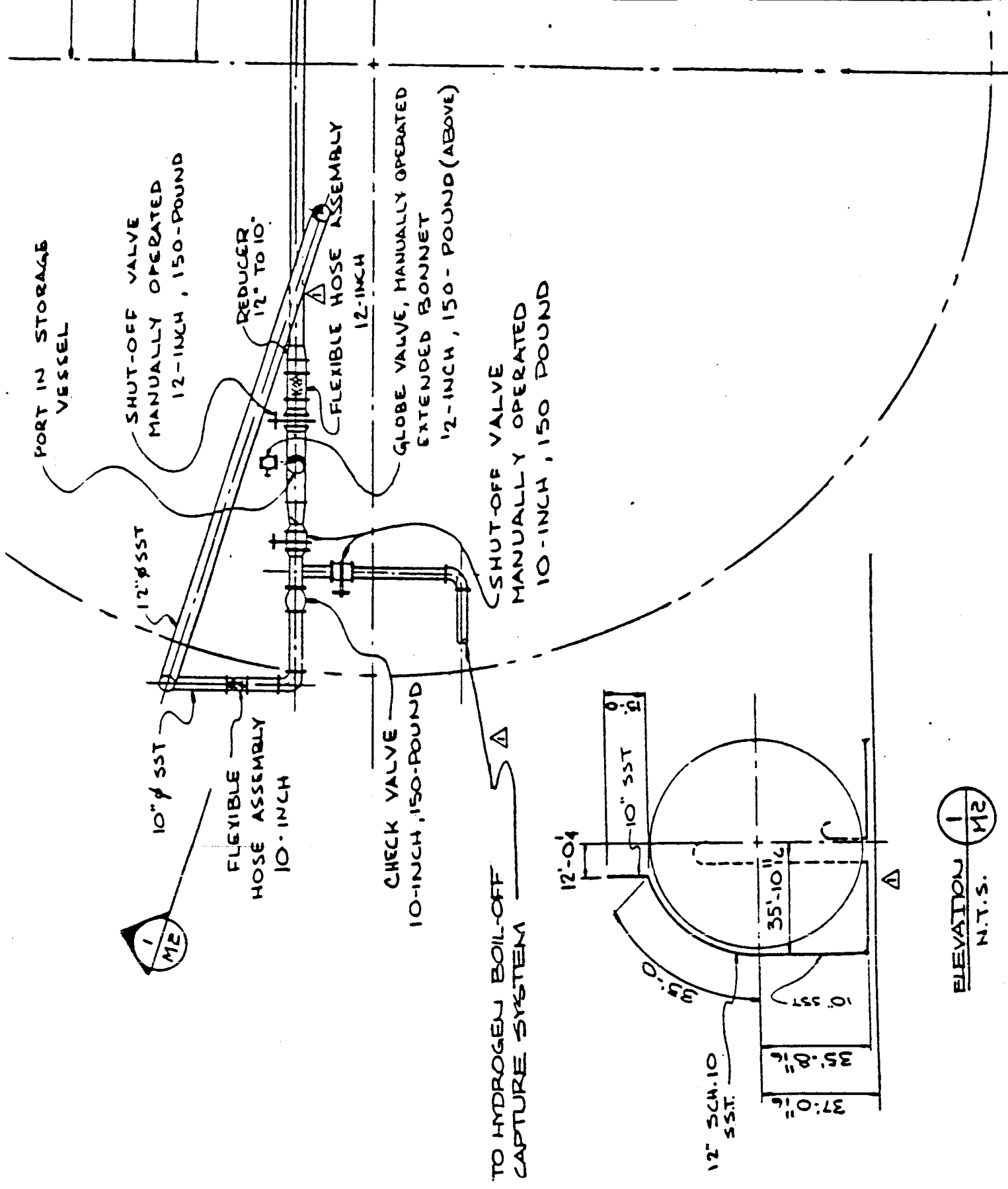


FIGURE 32: Detail of hydrogen recovery system connection point in existing piping. Ref. 5.

V. FINAL COMMENTS AND RECOMMENDATIONS

The program accomplished its stated mission; to demonstrate the technical feasibility of capturing low pressure hydrogen vapor as a reversible metal hydride at very rapid rates for subsequent reliquefaction. Based upon the results presented in this report, Ergenics believes the hydrogen capture system can be scaled directly for full scale operation. The extremely rapid absorption capability of metal hydrides suggests the alternative possibility of using a much smaller system operating on a short (3 to 5 minute) absorption/desorption cycle and acting as a staged compressor; the boiloff being stored as a compressed gas. Potential savings may be realized since at pressures as low as 1000 psi only fifteen tube trailers would be required to store all the gas for the slower reliquefaction process. Future work by Ergenics teamed with a suitable engineering construction firm should include:

1. An engineering analysis and cost study be done for each of the capture/reliquefaction scenarios identified.
2. Fabrication of a single full-scale component be completed for testing at the KSC on an actual LH₂ boiloff stream.
3. Based upon the single component test results, design improvements should be added and a complete system fabricated at one launch complex.
4. Similar systems to be constructed at other launch sites.

ACKNOWLEDGEMENTS

The authors; M. J. Rosso, Project Supervisor and P. M. Golben, Design Engineer, express their gratitude to Mr. J. Spears and Mr. F. Howard of NASA/KSC for their assistance in initiating this program and in gathering technical information. Our appreciation to Dr. E. L. Huston and Dr. G. D. Sandrock for their expertise and many helpful discussions regarding hydride alloy technical information. We also acknowledge the contributions of Mr. D. J. Hanley in the fabrication and testing of the demonstration device. Many thanks to Ms. Rosemarie Maslak and Ms. Barbara Tuthill for editing and typing the final report.

REFERENCES

1. Information supplied by Mr. Frank Howard, NASA Technical Representative.
2. Mr. Robert Gibbs and Dr. Richard Thomas of Cryogenic Consultants, Inc. with Mr. Lynn Terry, private consultant.
3. Goodell, P. D., Sandrock, G. D. and Huston, E. L., International Nickel Company, Inc. "Microstructure and Hydriding Studies of AB₅ Hydrogen Storage Compounds." January 1980 Final Report prepared for Sandia National Laboratories, SAND79-7095.
4. Goodell, P. D., Inco Alloy Products Company Research Center Project Report 3101.3, "Dynamic Hydriding Alloy Data", February 23, 1983.
5. G & H Engineering, Inc., Gilbertsville, PA.

APPENDIX A

CRYOGENIC CONSULTANTS REPORT

by

L. E. TERRY

RICHARD THOMAS

AND

ROBERT GIBBS

EDITED BY M. J. ROSSO

HYDROGEN RECOVERY, SIZING OF QUANTITY OF HYDROGEN VAPORIZED IN FILLING

The boiloff or vaporization of LH_2 as it is "off-loaded" from the tankers to the main storage Dewar at KSC is a product of the following four contributions.

1. Cooldown of the vacuum jacketed lines.
2. Boiloff from flashing of a high pressure liquid into a low pressure volume.
3. Boiloff from cooling down of dewar as liquid fills the dewar.
4. Ullage displacement.

Several steps are necessary in order to find the boiloff from each of the above contributions.

1. Find the equivalent length of piping of the fill lines to the dewar.
2. Determine the LH_2 flow rate from the known transfer line pressure.
3. Calculate the heat capacity, cool down time and boiloff based on the fill-line length determined in Step 1.
4. Determine the gas displaced from the dewar's ullage space as the liquid level rises in the dewar.
5. Estimate the liquid evaporated during the cool-down of the dewar walls. The temperature differential between the top and bottom of the dewar was assumed to be 5°K .
6. Calculate flashing into the dewar using the First Law of Thermodynamics and known states to determine the final quality of the liquid in the dewar.

The contributions are added and the total flow-rate as a function of liquid initially in the dewar may be determined.

The actual length of the vacuum fill line is approximately 178 feet. Also in the line are 1 flexible hose, 1 elbow, 2 relief valves, and 3 globe valves. These fittings are equal to about 66 equivalent elbows. The equivalent length of piping is, therefore, approximately 700 feet. (1). Using the equivalent length of piping and a known pressure drop between the line pressure and the dewar, the approximate mass flow rate of liquid can be determined.

The pressure drop (lb/ft²) in terms of viscosity, Reynold's number and mean fluid density is:

$$P = fL\mu^2 N_{Re}^2 / \rho g_c D^3 \quad (2) \quad \text{Eq 1}$$

where:

f is the coefficient of friction, dimensionless

L is the equivalent length, ft.

D is the inside diameter, 4 inch scd 5, ft.

μ is the viscosity, lbm/ft-sec.

N_{Re} is the Reynold's number, dimensionless

ρ is the mean density of the liquid, lbm/ft.³

g_c is the gravity conversion constant, ft/sec²

The same equation can be reduced to the following when known terms are substituted:

$$P = 2.2 \times 10^{-8} N_{Re}^2 / \mu \quad \text{Eq 2}$$

here the viscosity is 9.54×10^{-6} lbm/ft-sec. at 20° K.

Table I is a compilation of the results of the pressure drop calculations. The results were obtained by assuming a pressure drop, then guessing at a Reynold's number and getting the corresponding coefficient of friction. Using these numbers

in the pressure drop equation, the calculated results were checked to see if both sides of the equation were equal. If not, then a new Reynold's number was guessed at and the results checked. The iteration was continued until the correct Reynold's number was obtained for the pressure drop assumed. The mass flow rate of liquid hydrogen could then be determined from the following equation:

$$\dot{m} = N_{Re} \mu A / D \quad \text{Eq 3}$$

where:

\dot{m} is the mass flow rate, lbm/sec.

N_{Re} is the Reynold's number, dimensionless

μ is the viscosity, lbm/ft-sec.

A is the internal cross-sectional area of the pipe, ft.²

D is the internal diameter, ft.

Which is actually a rearrangement of the equation for computing the Reynold's number

$$N_{Re} = \dot{m} D / \mu A \quad \text{and as } A = \pi D^2 / 4$$

$$N_{Re} = 4 \dot{m} / \pi \mu D$$

The results of the pressure drop and mass flow rate calculation are given in Table I. The equivalent volume flow rate of the liquid if all liquid were converted to gas at standard conditions is given in column 4. Columns 5, 6 and 7 present the mean density of the liquid, the velocity of the liquid in the pipe and corresponding Mach number, respectively.

P		\dot{m}	Q	m	V	
PSIG	N_{Re}	lbm/sec	<u>SCFM</u>	<u>lbm/cu.ft.</u>	<u>ft/sec</u>	<u>M</u>
30	6.8E6	18.36	2.11E5	4.17	86.6	.077
25	6.2E6	16.74	1.93E5	4.21	78.2	.070
20	5.5E6	14.85	1.71E5	4.23	69.0	.062
15	4.7E6	12.69	1.46E5	4.25	58.7	.052
10	3.8E6	10.26	1.18E5	4.27	47.3	.042
7	3.2E6	8.64	9.95E4	4.27	39.8	.035
5	2.6E6	7.02	8.09E4	4.29	32.2	.028

TABLE I: Mass flow rate of liquid in the fill line as a function of differential pressure between the fill line and dewar.

The next thing to calculate is the cooldown of the vacuum jacketed piping. There are two contributions to the liquid boiloff as it first flows down the piping. One term is the steady state heat transfer through the insulation. Since the temperature varies from approximately ambient down to the liquid temperature, one-half of the steady state heat gain is used. The allowable heat gain by NASA specifications is 1000 BTU/hr for the dewar and 1800 BTU/hr for fill lines. (2) The external heat transfer gain is then about 1400 BTU/hr. Assuming that the cooldown time is about 5 minutes, the amount of heat transferred in that time is 1.2×10^5 Joules. This term will be shown to be negligible as compared to the sensible heat of the lines, which is the other contributing term to liquid boiloff during the cooldown of the transfer lines. The vacuum jacketed inner line is constructed of Schedule 5, 4 inch Invar pipe. The heat capacity for nickel as a function of temperature was obtained from the Handbook of Chemistry and Physics, 41st Ed. page 2273 (5). The heat capacity for iron is roughly the same as that for nickel. The data were fitted to a curve and over the range of 20-300K, the equation is:

$$C_p(T) = .0145 + 8.557 \times 10^{-4}T - 1.979 \times 10^{-6}T^2 + 1.536 \times 10^{-9}T^3 \text{ cal/g-K}$$

The average sensible heat capacity over the temperature range of 20-300 K is 0.070 cal/g-K.

The length of tubing is about 178 feet and the mass of metal per foot is 3.915 lbm/ft for Schedule 5, 4 inch pipe. Allowing 25% extra for supports, valve bodies and getter material, the mass used to determine the heat capacity was 870 lbm. The amount of energy needed to cool down this mass is 3.27×10^7 Joules. This amount is more than a factor of one hundred greater than the heat leak from ambient. Using the calculated heat capacity and the external heat gain, it would take about 2.8 days for the transfer lines to warm up to ambient temperature.

A calculation must be done to find the mass of liquid required to cool down the fill line and also find the time required to cool the line down. To find the

time to cool down the line, it is assumed that the boiloff is so fast that choked flow is reached in the line, which is normally the case. The calculation is based on a 4 inch line with a discharge coefficient of 0.60 and a cross-sectional area of 0.020 sq. ft. at the exit of the fill line. The equation for the velocity of the choked flow is:

$$V = C_d (\gamma g_c R T_g)^{1/2}$$

where:

V is the velocity, m/sec.

C_d is the discharge coefficient, dimensionless

γ is the ratio of C_p/C_v , dimensionless

g_c is the gravity conversion coefficient, m/sec.²

R is the Gas Constant for hydrogen, m-Kg/Kg-°K

T_g is the average gas temperature, °K

At 1.17 atmospheres pressure and 160 K the density of hydrogen is 16.77×10^{-5} g/cc. The mass flow rate of hydrogen gas is therefore .197 lbm/sec or 5.83×10^3 gm/min at choked flow conditions. This is equivalent to 2.27×10^3 SCFM. The time that this flow is taking place is only for the amount of time that it takes to cool down the fill lines. Time to cool down the line is given by the following equation:

$$t_{SS} = (\Sigma \dot{m} (T_i - T_{SS}) C_p - V (\rho_{SS} (\mu_{SS} - H_f) = \rho_i (\mu_i - H_f)) / (m_g (H_g - H_f) - 0.5 Q_{SS})$$

where:

t_{SS} is the time to reach steady state, sec.

$\dot{m}(T_i - T_{SS})C_p$ is the energy to cool down the fill line due to heat capacity, Joules

V is the volume of the line, cc

ρ_{SS} and ρ_i are the steady state and initial densities in the line, g/cc

u_{SS} and u_i are the steady state and initial internal energies of the hydrogen, J/g

H_f is the enthalpy of the hydrogen liquid at steady state, J/g

m_g is the mass flow rate of hydrogen gas calculated at choked flow, g/sec

H_g is the enthalpy calculated for the hydrogen gas at the average temperature in the line, J/g

Q_{SS} is the steady state heat gain, cal/sec.

It was assumed that the quality did not change very much for the liquid and was considered to be zero. Doing this, the states necessary to complete the above equation are:

$$\rho_{SS} = .0663 \text{ g/cc at 2.5 atm. sat. liquid}$$

$$H_f = -219.6 \text{ J/g at 2.5 atm. sat. liquid}$$

$$u_{SS} = -223.4 \text{ J/g at 2.5 atm. sat. liquid}$$

$$\rho_i = 8.18 \times 10^{-5} \text{ g/cc at 1 atm. and 300 K}$$

$$u_i = 2.989 \times 10^3 \text{ J/g at 2.5 atm. and 160 K}$$

$$H_g = 2.012 \times 10^3 \text{ J/g at 2.5 atm. and 160 K}$$

Substituting these into the equation for time to reach steady state, the result is 1.47 minutes.

One more equation is needed and that is the mass of liquid hydrogen needed to cool down the fill piping. It is as follows:

$$M_f/M_w = C_w (T_i - T_{ss}) / (H_g - H_f) + V (\rho_{ss} - \rho_i) / M_w + Q_{ss} t_{ss} / (2 M_w (H_g - H_f))$$

where:

M_f/M_w is the lbm of liquid hydrogen needed per lbm of metal

The rest of the terms are as above. Substituting the necessary values the mass of hydrogen needed per lbm of metal is .209 lbm H_2 / lbm metal.

The pressurization of the dewar can be calculated from the saturation rule given on page 475 of Barron. This rule, especially for hydrogen is in error on the liberal side, but for lack of information, this rule will serve well enough since the time to pressurize is on the order of only a few minutes. The saturation rule is the difference in the volume times density at the initial and final states.

$$M_g = V_{g2} \rho_{g2} - V_{g1} \rho_{g1}$$

where m_g is the change in mass of the gas from state 1 to 2

V_{g2} and V_{g1} are the volumes the gas occupies at states 1 and 2 respectively

ρ_{g2} and ρ_{g1} are the densities of the gas at states 1 and 2 respectively

In terms of the number of gallons of the system, the volumes can be written as follows:

$$V_{g2} = 1.13 \times 10^5 - 0.134V$$

$$V_{g1} = 1.13 \times 10^5 - (V + 55,000) 0.134$$

where V is the initial volume of liquid in the dewar

The saturation rule can then be written as

$$m_g = (1.13 \times 10^5 - 0.134V) \rho_{g2} - (1.13 \times 10^5 - 0.134(V + 55,000)) \rho_{g1}$$

The time to pressurize can be determined by the maximum flow rate of liquid into the dewar as a function of the pressure drop. This is where much of the error comes in. The liquid must be able to flash entirely into vapor or be boiled off by heat transfer. The time to pressurize is given by

$$t = 191.8 \text{mg} / \dot{Q}_t$$

where:

\dot{Q}_t is the volume flow rate based on the pressure drop, SCFM

Table II gives the results of the saturation rule for a pressure drop of 20 psig and pressurizing from 1 atm to 1.17 atm.

Volume Gallon	Mass, M_g lbm	Q SCF	Time Min
100,000	664	1.27E5	0.745
200,000	615	1.18E5	0.690
300,000	567	1.09E5	0.636
400,000	519	9.95E4	0.582
500,000	471	9.03E4	0.528
600,000	422	8.10E4	0.473
700,000	374	7.18E4	0.419
750,000	350	6.71E4	0.392

TABLE II Pressurization of the dewar from 1 atm at a pressure flow rate of 20 psig.

Another contribution to the boiloff is the heat capacity of the dewar walls. On page 450 of Barron, an equation is given to determine the minimum thickness necessary for the walls of an elliptical shape. For a sphere, the minor diameter is the same as the major diameter. The equation for the thickness is:

$$t_h = PDK / (2S_a E_w - 0.2P)$$

where:

P is the maximum operating pressure

D is the diameter, ft.

$K = 0.167 (2 + (D/D_1)^{1/2})$ and D/D_1 is 1 for a sphere

S_a is the allowable stress, psi

E_w is the weld efficiency, per cent

P is assumed to be 75 psia, D is 60.5 ft.. S_a is 18,750, and E_w is 100. Substituting these values into the equation, one obtains for the minimum thickness of 0.71 in. Using the density of steel of 7.84 g/cc and finding the net volume of the dewar wall, the mass of the inner wall is 9.3×10^8 gm.

An equation for the internal volume of a sphere as a function of the height from the bottom of the sphere and the radius of a sphere is:

$$V = 0.33\pi h^2 (3R - h)$$

This equation can be written as a cubic equation in h with the radius as 30.25 ft. and V in gallons, the equation is

$$h^3 - 90.75 h^2 + 0.12766V = 0$$

The surface area of the sphere at this height can also be written as a function of the radius and the height. It is

$$S = 2\pi R h$$

Table III shows the amount of hydrogen boiled off as a function of the volume of liquid initially in the sphere. The calculations iterate to find the height necessary to solve the cubic equation and then the surface area is calculated. The net difference in going from one liquid level to another in increments of 50,000 gallons is given and the net surface area covered by liquid as it is filled to the next higher level is determined. The mass of steel knowing the wall thickness can then be calculated and the energy to cool it down 5 K is then arrived at. The mass of hydrogen boiled off can then be determined and the rate in SCFM is taken over 60 minutes.

V, gal	h, ft.	A, ft ²	A, ft ²	m steel, gm	Q, Joules	m, H ₂	SCFM
50,000	8.82	1676	1676	2.32E7	2.9E7	3.25E4	228
100,000	12.80	2433	757	1.05E7	1.31E7	1.47E4	103
150,000	16.01	3043	610	8.46E6	1.06E7	1.18E4	83
200,000	18.84	3581	538	7.46E6	9.33E6	1.04E4	73
250,000	21.46	4079	498	6.91E6	8.64E6	9.67E3	68
300,000	23.94	4550	471	6.53E6	8.16E6	9.14E3	64
350,000	26.34	5006	456	6.33E6	7.91E6	8.86E3	62
400,000	28.68	5453	447	6.21E6	7.76E6	8.60E3	61
425,000	29.85	5673	220	3.05E6	3.81E6	4.27E3	30
450,000	31.02	5893	220	3.05E6	3.81E6	4.27E3	30
500,000	33.36	6340	447	6.21E6	7.76E6	8.60E3	61
550,000	35.76	6796	456	6.33E6	7.91E6	8.86E3	62
600,000	38.24	7266	471	6.53E6	8.16E6	9.14E3	64
650,000	40.86	7765	498	6.91E6	8.64E6	9.67E3	68
700,000	43.69	8303	538	7.46E6	9.33E6	1.04E4	73
750,000	46.90	8913	610	8.46E6	1.06E7	1.18E4	83
800,000	50.88	9670	757	1.05E7	1.31E7	1.47E4	103
850,000	60.25	11346	1676	2.32E7	2.90E7	3.25E4	228

TABLE III. Boiloff from cooling down the heat capacity of the dewar.

The largest contribution to boiloff is from flashing of the higher pressure liquid to partial vapor into the low pressure dewar. An example of how to determine this is given in Van Wylen and Sonntag on page 122. (6) The First Law of Thermodynamics is used to find the state of the hydrogen in the dewar. The calculations were done twice; once using MKS units and once using English units. The results would be identical except that for the English calculation, I used the viscosity value of 9.54×10^{-6} lbm/ft-sec obtained from Scott. (4) In the MKS calculation, I used a value of 1.07×10^{-5} Pa-sec taken from a graph reprinted from Chapter II of Technology and Uses of Liquid Hydrogen. (7) The value 1.07×10^{-5} Pa-sec equals only 7.19×10^{-6} lbm/ft-sec, and, therefore, the results do not agree exactly with each other. They are, however, in exact agreement when the friction factor is limited to a minimum value at high Reynold's numbers

The mass flow is given by: (8)

$$\dot{m} = (\pi^2 \rho \Delta P D^5 / 8 f L)^{1/2}$$

Friction factors were needed in order to calculate the flow. Barron gives friction factor equations on page 135 for smooth pipes, but the equations he gives are only for Reynold's numbers less than 3×10^6 . (4) The reason for limiting the range for the validity of the equations can be seen from an examination of charts of friction factor versus Reynold's number as in "Flow of Fluids through Valves, Fittings, and Pipe, Technical Paper No. 410," (Crane Company), pp. A-24 and A-25. (9)

For all pipes, the friction factor levels off to a constant value at high Reynold's numbers. This constant minimum value depends on the relative roughness of the pipe. For very smooth pipes such as drawn tubing, the minimum will be 0.0085 to 0.0095 for 4 inch tubing at Reynold's numbers of 3×10^8 and greater. But for commercial steel pipe, the minimum will be about 0.016 for Reynold's number greater than 2×10^6 . If the pipe in question has the roughness of commercial steel rather than drawn tubing, the Reynold's numbers of the mass flow are in this "minimum value" range and Barron's friction factor equations are not valid.

The mass flows were calculated using several assumptions:

- 1) The friction factor equations are valid for all Reynold's numbers,
- 2) the friction factor reaches a minimum value of 0.0098 at Reynold's numbers $>3 \times 10^6$,
- 3) The limiting minimum value is 0.016 instead of 0.0098.

The analysis assumes that the hydrogen state point moves along the saturated-liquid curve as it is transferred, that is, the hydrogen is at the boiling point appropriate for the pressure at that location. We will assume that the tanker pressure is 22.5 psig and that the hydrogen enters the transfer line as a liquid (the quality or ratio of mass of vapor to the total mass flow is zero at the tanker end of the pipe). As the liquid flows along, the pressure falls, finally reaching 2.5 psig at the storage tank. Since the pressure falls, the boiling point decreases so some of the fluid becomes liquid at this new lower boiling point and lower enthalpy while part of it is vaporized to a gas, also at this new lower temperature but with an enthalpy greater by the heat of vaporization. There would be no net enthalpy change if there were not heat leak in the transfer line, no change in the potential energy of the gas, and no change in the velocity of fluid along its path.

If there are elevations, some of the pressure drop goes into raising the potential energy of the fluid. We will show later that the heat leak of about 300W causes little additional vaporization of the hydrogen as compared to the pressure drop itself. Finally, since part of the fluid does change to vapor in the pipe, the mean density of the exiting hydrogen is less than that of the entering hydrogen. Thus, to conserve mass flow, the hydrogen must exit at a higher velocity than it enters. The increase in kinetic energy required "uses up" some of the pressure drop and leads to less liquid going to vapor.

From Barron,

$$X_2 = \frac{\int_1^2 \left(\frac{dh}{dP} \right)_{\text{sat}} dP - \frac{V_2^2 - V_1^2}{2} - g (Z_2 - Z_1) + \frac{Q}{\dot{m}}}{h_{fg2}}$$

NOTE: I decided to use "V" for velocity and "v" for specific volume

where:

X_2 = quality of hydrogen at exit,

$\frac{dh}{dp}_{\text{sat}}$ = change in enthalpy of the liquid for a change in pressure along the saturated-liquid curve,

V_2 = velocity of exiting vapor and liquid, ft/sec.

V_1 = velocity of entering liquid, ft/sec.

$(Z_2 - Z_1)$ = net change in elevation, ft.

\dot{Q} = heat leak into transfer line, BTU/hr.

\dot{m} = mass flow rate, lb/hr.

h_{fg2} = latent heat of vaporization for conditions at exit, BTU/lb

In Figure 1, I have plotted (dh/dp) versus P for liquid hydrogen over the range of interest. The data are from NBS Monograph 94.(9). For this example, the transfer conditions will be assumed to be $P_1 = 22.5 \text{ psig} = 2.53 \text{ atm}$, $P_2 = 2.5 \text{ psig} = 1.17 \text{ atm}$. Therefore $\Delta P = 20 \text{ psi} = 1.361 \text{ atm}$. The first term in the numerator is just the area under the dh/dp curve over the region $1.17 < P < 2.53$. This area was approximated by taking ΔP times the value of dh/dp at the midpoint, $\sim 25.5 \text{ J/g atm}$, giving 34.7 J/g .

We will assume net elevation changes to be zero. The velocity change can not yet be calculated - we must iterate to get a final answer. $\dot{Q} = 1000 \text{ BTU/hr} = 293 \text{ Watts}$, so the last term in the numerator is 293 W/m . If $\dot{m} \sim 8 \text{ kg/s}$, then $\dot{Q} = 0.04 \text{ J/s}$ and is completely negligible for this high mass flow rate.

Then, as a first approximation,

$$X_2 = \frac{34.7 \text{ J/g}}{443 \text{ J/g}} = 0.0783$$

If, however, 7.83% of the transferred mass flashes to vapor, the mean density of the exiting liquid and vapor will be much less than the density of the liquid entering the transfer line. In order to conserve mass flow, the velocity of the exiting fluid must be greater than that of the entering liquid.

$$\rho_2 = \frac{1}{v_{m2}} = \frac{1}{(1-X_2) v_{f2} + X_2 v_{g2}}$$

where:

v_{m2} = the mean specific volume at exit,

v_{f2} = liquid specific volume at $P = 2.5 \text{ psig}$, $T = T_{\text{sat}}$, l/kg

v_{g2} = vapor specific volume at exit conditions, l/kg

Thus

$$\rho_2 = \frac{1}{(0.9217)(14.254) + (0.0783)(652.9)} = \frac{1}{64.26} \text{ g/cm}^3$$

$$\rho_2 = 0.01556 \text{ g/cm}^3 = 15.56 \text{ g/l} = 15.56 \text{ kg/m}^3$$

Since the initial density was 66.21 kg/m^3 , the velocity change is larger.

As $v = \dot{m}/(\rho_1 A)$, $v_1 = 12.69 \text{ m/s}$ for a mass flow rate of 8 kg/s .

$$\text{Thus } V_2 = \frac{\rho_1}{\rho_2} v_1 = 4.255 V_1 = 54 \text{ m/s}$$

$$v_2^2 - v_1^2 = 1377 \text{ J/kg} = 1.377 \text{ J/g.}$$

The energy of 1.4 J/g is required to increase the momentum of the fluid and is supplied by part of the pressure drop. There is then less energy available to

provide the heat of vaporization of the liquid hydrogen.

Our second approximation is kthen,

$$X_2 = \frac{34.7 \text{ J/g} - 1.4 \text{ J/g}}{443 \text{ J/g}} = 0.0752$$

We proceed in this manner and obtain the results shown in Table IV. We see the result converges to 0.0754 in three iterations.

Iteration	Kinetic Energy Change (J/g)	(kg/m ³)	x ₂
0	0.00	66.21	0.0783
1	1.38	15.56	0.0752
2	1.29	16.06	0.0754
3	1.29	16.02	0.0754

TABLE IV: Results of iterative calculation for quality of hydrogen at exit.

Discussion of flashing results

The results show that the density of the exiting hydrogen is only 24% of the density of the entering fluid. The kinetic energy change required uses 4.85 psi of the 20 psi pressure drop. This implies that the mass flow calculations done in the first part of their report could be greatly in error since, for a pressure drop of 20 psi, only ~15 psi are available to overcome the friction losses. But more importantly, the assumption that the flow could be calculated using only the properties of the fluid (density and viscosity) is invalid. In fact, whereas every gram of entering hydrogen consisted of 15.1 cc of liquid, every gram of exiting hydrogen consists of only 13.2 cc of liquid plus 49.2 cc of vapor. Moreover, the flashing results depend on

the validity of the homogeneous model which requires bubble flow. In the example in Barron the vapor was only about 20% of the exiting volume. In our case, it is nearly 80% of the exiting volume. The problem is really one of two-phase flow because of the large amount of flashing produced by the 20 psi pressure drop.

Since the mass flow and flashing results are mutually interdependent, the results obtained above are not completely valid. The effect of flashing is to reduce the mass flow rate. The effect of the mass flow rate on the amount of flashing is to increase the amount due to the heat leak into the transfer line. Also, the kinetic energy term will be smaller, but as seen in Table IV, this is a small effect. Since the amount of flashing depends mostly on the total pressure drop (frictional pressure drop plus momentum pressure drop), this value will probably not change much as long as the 20 psi drop is maintained during the transfer and as long as the flow remains mixed, i.e., the liquid and vapor don't stratify.

If we use the average density, 41.12 kg/m^3 , and assume the flow is still fully turbulent so that the friction factor has bottomed out at a value of 0.015, then after a few iterations we find

$$\rho_2 = 15.75 \text{ kg/m}^3, \rho_{\text{avg}} = 40.98 \text{ kg/m}^3$$

$$\Delta P (\text{frictional}) = 17.7 \text{ psi}, \Delta P (\text{momentum}) = 2.3 \text{ psi}$$

$$\dot{m} = 5.40 \text{ kg/s}, \text{ and } X_2 = 0.0771$$

Therefore 416 g/s would be produced by flashing, corresponding to

$$\frac{(416 \text{ g/s})(60 \text{ s/m})}{2.362 \text{ g/ft}^3} = 10,570 \text{ SCFM}$$

where a standard cubic foot is taken to be at 1 atm and 70°F

If the flow stratifies, the vapor and liquid may exit at different velocities. To handle that situation one might attempt to write down a set of

equations describing the flow at different segments along the length of the pipe and match the end points of each segment. In any case, the flowing hydrogen is going to undergo a pressure drop, so, for a 20 psig drop, ~7% - 8% of the mass of hydrogen leaving the tankers will arrive at the storage vessel as vapor. Knowing this, it is probably easier just to empirically determine the mass flow rate by measuring the time it takes to fill up the storage vessel. Then the rate at which gas will be vented during the transfer (as a result of flashing) can be calculated.

Note that these results are a worst case since the tankers arrive with a pressure of only 5-10 psig and are then pressurized into 22.5 psig. The hydrogen is, therefore, not on the saturation curve when the transfer begins but is instead at some temperature below the boiling point at $P = 22.5$ psig. To compute the flashing losses one needs to plot dh/dP versus P for the liquid in going from its bulk temperature in the tanker to its boiling point at 2.5 psig in the vessel.

As the transfer proceeds, the liquid hydrogen in the tanker will warm through heat inleak, and the flashing losses will increase. If the heat transfer through the tanker insulation is known, the time required for the hydrogen to reach the boiling point can be calculated. (The heat capacity of the liquid hydrogen is about 11 J/(g-k) for the conditions in the tanker.)

The amount of liquid needed to cool down the transfer line depends upon what happens to the "hot" gas that exits the transfer line during this process. Perhaps there are valves which allow the gas to be vented directly until the transfer line is cold, and then the valves are reconfigured to allow the fluid to enter the storage vessel.

If this is not the case, then one must compute how much liquid hydrogen will be boiled off when the storage vessel is not empty. If it is empty, then the amount of hydrogen required to cool the storage vessel down must be computed. In the former case, the amount of hydrogen that will be evaporated by the hot gas arriving at the beginning of the transfer will depend on the details of the construction. If there is a phase separator or vapor diffuser, the warm gas will be directed away from the surface of the cold liquid so that it vents before transferring much of its heat to the liquid hydrogen already in the vessel.

One of the last things needed to know in designing a hydride storage vessel is the temperature of the hydrogen entering the storage vessel. If the hydrogen is cold, this will provide some cooling to the storage beds. To find the temperature, the external heat gain from the ambient air must be calculated and equated to the heating of an equivalent mass of hydrogen.

Three resistances are needed to find the external heat transfer rate. They are the external heat transfer coefficient, the internal heat transfer coefficient, and the resistance due to the conductivity of the pipe. The external heat transfer coefficient is assumed to be 20 BTU/hr-sq.ft-F for lack of better information. This is about midrange for a natural convection coefficient. The internal coefficient is more difficult to estimate. Since it depends on the temperature at which the properties of the hydrogen gas exist. If the bulk temperature of the hydrogen gas is used, then curves, iterations, or tables of values must be made to find where the external heat transfer from ambient temperature equals the sensible heating of the hydrogen. This varies directly with the mass flow rate of the hydrogen.

The external heat transfer coefficient can be found from the following equation of the Nusselt Number:

$$N_{nu} = 0.021 N_{pr}^{0.6} N_{re}^{0.8}$$

where:

N_{nu} is the Nusselt number

N_{pr} is the Prandtl number

and N_{re} is the Reynold's number

The Nusselt number is equal to the heat transfer coefficient times the internal diameter of the pipe divided by the conductivity of the hydrogen gas. The Prandtl number for hydrogen is about 0.7 over a wide temperature range. Using this number and solving for the heat transfer coefficient:

$$h(t) = [0.01695 k(t)/D] [VD/v(t)/\mu(t)]^{0.8}$$

where:

$h(t)$ is the external heat transfer coefficient

D is the diameter, ft.

$k(t)$ is the conductivity of the hydrogen gas as a function of temperature

V is the velocity of the hydrogen gas, ft/sec.

$v(t)$ is the specific volume of the hydrogen gas as a function of temperature, ft³/lbm

$\mu(t)$ is the viscosity of the hydrogen gas as a function of temperature, lbm/ft-sec.

The external heat transfer is then equal to the following equation:

$$Q = 1.8(300-t)/1/(2\pi \cdot 0.434h(t)L) + 1/(2\pi \cdot 0.441(20L) + \ln(1.016)/(2\pi k(t)L))$$

Equations for the variables that are a function of temperature have been fitted to data using a least squares method. Since units for data varied, equations were fitted to the data as it was and then conversion factors were used in the final equation to get the correct result.

Ptanker (psig)	Pdrop (psig)	Mass Flow (lbm/s)	Mass Flow (kg/s)	Density (lbm/ft ³)	Friction Factor	Reynolds Number	Velocity (ft/s)
15.50	13.00	17.57	7.97	4.212	0.0089	6490678	40.710
16.50	14.00	18.25	8.28	4.201	0.0089	6742245	42.396
17.50	15.00	18.90	8.57	4.190	0.0088	6984411	44.032
18.50	16.00	19.53	8.86	4.179	0.0088	7218048	45.622
19.50	17.00	20.15	9.14	4.169	0.0088	7443896	47.170
20.50	18.00	20.74	9.41	4.158	0.0087	7662590	48.682
21.50	19.00	21.31	9.67	4.147	0.0087	7874680	50.159
22.50	20.00	21.87	9.92	4.136	0.0087	8080645	51.605
23.50	21.00	22.41	10.17	4.126	0.0087	8280907	53.021
24.50	22.00	22.94	10.40	4.115	0.0086	8475838	54.411
25.50	23.00	23.45	10.64	4.104	0.0086	8665770	55.776
26.50	24.00	23.95	10.87	4.093	0.0086	8851000	57.118
27.50	25.00	24.44	11.09	4.083	0.0086	9031794	58.438
28.50	26.00	24.92	11.30	4.072	0.0086	9208394	59.738
29.50	27.00	25.39	11.52	4.061	0.0085	9381018	61.019
30.50	28.00	25.84	11.72	4.050	0.0085	9549865	62.282

TABLE V. Result of calculation using English units. Friction factor fit assumed valid for all Reynold's numbers

Ptanker (psig)	Pdrop (psig)	Mass Flow (kg/s)	Mass Flow (lbm/s)	Density (kg/m ³)	Friction Factor	Reynolds Number	Velocity (m/s)
14.50	12.00	7.781	17.15	67.637	0.0086	8409846	12.086
15.50	13.00	8.107	17.87	67.465	0.0086	8762248	12.625
16.50	14.00	8.420	18.56	67.293	0.0086	9100562	13.146
17.50	15.00	8.721	19.23	67.121	0.0085	9426193	13.651
18.50	16.00	9.011	19.87	66.948	0.0085	9740321	14.142
19.50	17.00	9.292	20.49	66.776	0.0085	10043945	14.621
20.50	18.00	9.564	21.09	66.604	0.0084	10337924	15.088
21.50	19.00	9.828	21.67	66.432	0.0084	10622998	15.544
22.50	20.00	10.084	22.23	66.259	0.0084	10899817	15.990
23.50	21.00	10.333	22.78	66.087	0.0084	11168948	16.428
24.50	22.00	10.576	23.31	65.915	0.0084	11430895	16.857
25.50	23.00	10.812	23.84	65.743	0.0083	11686107	17.279
26.50	24.00	11.042	24.34	65.570	0.0083	11934983	17.693
27.50	25.00	11.267	24.84	65.398	0.0083	12177884	18.101
28.50	26.00	11.486	25.32	65.226	0.0083	12415134	18.502
29.50	27.00	11.701	25.80	65.054	0.0083	12647030	18.897
30.50	28.00	11.910	26.26	64.881	0.0083	12873830	19.287
31.50	29.00	12.116	26.71	64.709	0.0082	13095805	19.672
32.50	30.00	12.317	27.15	64.537	0.0082	13313155	20.052

TABLE VI. Result when the friction factor is not limited even though fit may not be valid, MKS units.

Ptanker (psig)	Pdrop (psig)	Mass Flow (lbm/s)	Mass Flow (kg/s)	Density (lbm/ft ³)	Friction Factor	Reynolds Number	Velocity (ft/s)
15.50	13.00	16.72	7.58	4.212	0.0098	6177996	38.746
16.50	14.00	17.33	7.86	4.201	0.0098	6403020	40.260
17.50	15.00	17.91	8.12	4.190	0.0098	6619267	41.727
18.50	16.00	18.48	8.38	4.179	0.0098	6827572	43.151
19.50	17.00	19.02	8.63	4.169	0.0098	7028641	44.536
20.50	18.00	19.55	8.87	4.158	0.0098	7223078	45.886
21.50	19.00	20.06	9.10	4.147	0.0098	7411405	47.205
22.50	20.00	20.55	9.32	4.136	0.0098	7594077	48.494
23.50	21.00	21.03	9.54	4.126	0.0098	7771493	49.756
24.50	22.00	21.50	9.75	4.115	0.0098	7944004	50.994
25.50	23.00	21.95	9.96	4.104	0.0098	8111923	52.208
26.50	24.00	22.39	10.16	4.093	0.0098	8275531	53.401
27.50	25.00	22.83	10.35	4.083	0.0098	8435077	54.574
28.50	26.00	23.25	10.54	4.072	0.0098	8590789	55.728
29.50	27.00	23.66	10.73	4.061	0.0098	8742871	56.865
30.50	28.00	24.06	10.91	4.050	0.0098	8891510	57.985

Table VII: Friction factor limited to values of 0.0098 or larger. In English units.

Ptanker (psig)	Pdrop (psig)	Mass Flow (kg/s)	Mass Flow (lbm/s)	Density (kg/m ³)	Friction Factor	Reynolds Number	Velocity (m/s)
14.50	12.00	7.295	16.08	67.637	0.0098	7885622	11.332
15.50	13.00	7.583	16.72	67.465	0.0098	8197158	11.810
16.50	14.00	7.868	17.33	67.293	0.0098	8495727	12.271
17.50	15.00	8.125	17.91	67.121	0.0098	8782651	12.718
18.50	16.00	8.381	18.48	66.948	0.0098	9059037	13.152
19.50	17.00	8.627	19.02	66.776	0.0098	9325821	13.575
20.50	18.00	8.866	19.55	66.604	0.0098	9583806	13.986
21.50	19.00	9.097	20.06	66.432	0.0098	9833685	14.388
22.50	20.00	9.322	20.55	66.259	0.0098	10076059	14.781
23.50	21.00	9.539	21.03	66.087	0.0098	10311460	15.166
24.50	22.00	9.751	21.50	65.915	0.0098	10540353	15.543
25.50	23.00	9.957	21.95	65.743	0.0098	10763154	15.913
26.50	24.00	10.158	22.39	65.570	0.0098	10980233	16.277
27.50	25.00	10.354	22.83	65.398	0.0098	11191925	16.634
28.50	26.00	10.545	23.25	65.226	0.0098	11398528	16.986
29.50	27.00	10.732	23.66	65.054	0.0098	11600315	17.332
30.50	28.00	10.914	24.06	64.881	0.0098	11797533	17.674
31.50	29.00	11.093	24.45	64.709	0.0098	11990488	18.011
32.50	30.00	11.267	24.84	64.537	0.0098	12179145	18.343

TABLE VIII: Result when the friction factor is limited to values of 0.0098 or greater, in MKS units.

Ptanker (psig)	Pdrop (psig)	Mass Flow (lbm/s)	Mass Flow (kg/s)	Density (lbm/ft ³)	Friction Factor	Reynolds Number	Velocity (ft/s)
15.50	13.00	13.10	5.94	4.212	0.0160	4842323	38.369
16.50	14.00	13.58	6.16	4.201	0.0160	5018697	31.556
17.50	15.00	14.04	6.37	4.190	0.0160	5188193	32.706
18.50	16.00	14.48	6.57	4.179	0.0160	5351463	33.822
19.50	17.00	14.91	6.76	4.169	0.0160	5509061	34.907
20.50	18.00	15.32	6.95	4.158	0.0160	5661461	35.966
21.50	19.00	15.72	7.13	4.147	0.0160	5809072	36.999
22.50	20.00	16.11	7.31	4.136	0.0160	5952251	38.010
23.50	21.00	16.48	7.48	4.126	0.0160	6091309	38.999
24.50	22.00	16.85	7.64	4.115	0.0160	6226523	39.969
25.50	23.00	17.21	7.80	4.104	0.0160	6358139	40.921
26.50	24.00	17.55	7.96	4.093	0.0160	6486375	41.856
27.50	25.00	17.89	8.12	4.083	0.0160	6611428	42.775
28.50	26.00	18.22	8.27	4.072	0.0160	6733475	43.680
29.50	27.00	18.54	8.41	4.061	0.0160	6852677	44.571
30.50	28.00	18.86	8.55	4.050	0.0160	6969188	45.449

TABLE IX: Friction factor limited to values of 0.016 or larger in English Units.

Ptanker (psig)	Pdrop (psig)	Mass Flow (kg/s)	Mass Flow (lbm/s)	Density (kg/m ³)	Friction Factor	Reynolds Number	Velocity (m/s)
14.50	12.00	5.718	12.61	67.637	0.0160	6180764	8.882
15.50	13.00	5.944	13.10	67.463	0.0160	6424946	9.257
16.50	14.00	6.160	13.58	67.293	0.0160	6658963	9.618
17.50	15.00	6.368	14.04	67.121	0.0160	6883856	9.969
18.50	16.00	6.569	14.48	66.948	0.0160	7100488	10.309
19.50	17.00	6.762	14.91	66.776	0.0160	7309594	10.640
20.50	18.00	6.949	15.32	66.604	0.0160	7511804	10.962
21.50	19.00	7.130	15.72	66.432	0.0160	7707659	11.277
22.50	20.00	7.306	16.11	66.259	0.0160	7897632	11.585
23.50	21.00	7.477	16.48	66.087	0.0160	8082139	11.887
24.50	22.00	7.643	16.85	65.915	0.0160	8261546	12.183
25.50	23.00	7.804	17.21	65.743	0.0160	8436178	12.473
26.50	24.00	7.962	17.55	65.570	0.0160	8606325	12.758
27.50	25.00	8.115	17.89	65.398	0.0160	8772249	13.038
28.50	26.00	8.265	18.22	65.226	0.0160	8934185	13.314
29.50	27.00	8.411	18.54	65.054	0.0160	9092346	13.585
30.50	28.00	8.554	18.86	64.881	0.0160	9246926	13.853
31.50	29.00	8.694	19.17	64.709	0.0160	9398102	14.117
32.50	30.00	8.831	19.47	64.537	0.0160	9546034	14.377

TABLE X: Result when the friction factor is limited to values of 0.016 or greater. MKS units.

```

10      Calculate Mass Flow
20      12 September 1983
30      OPTION BASE 1
40      INPUT "Which printer?",Prt
50      PRINTER IS Prt
60      D=4.334*.0254
70      L=700.*.3048
80      Visc=.1*1.07E-4
90      Rho2=1.E+3+2.01594/29.82
100     Rho3=1.E+3+2.01594/30.98
110     A=PI*D*D/4.
120     PRINT USING "K";"Ptanker Pdrop Mass Mass Density Friction Reynol
ds Velocity"
130     PRINT USING "K";" Flow Flow Factor Numbe
r "
140     PRINT USING "K";" (psig) (psig) (kg/s) (lbm/s) (kg/m3)
(m/s)"
150     PRINT
160     IMAGE DDD.DD,2X,DDD.DD,2X,DD.DDD,3X,DD.DD,2X,DDD.DDD,3X,Z.DDDD,3X,8D,3X,DD
D.DDD
170     FOR Pcar=14.5 TO 33
180         Pdrope=Pcar-2.5
190         Pdrop=6894.757*Pdrope
200         Rho=Rho2+(Rho3-Rho2)*(((Pcar+14.695949)/14.695949)-2)
210         Re=1.E+5
220         GOSUB Fric
230         Mflw=SQR(PI*PI*Rho*D*D*D*D*Pdrop/(8.*F*L))
240         REPEAT
250             Mflw0=Mflw
260             Re=4.*Mflw/(PI*Visc*D)
270             GOSUB Fric
280             Mflw=SQR(PI*PI*Rho*D*D*D*D*Pdrop/(8.*F*L))
290             UNTIL ABS((Mflw-Mflw0)/Mflw)<1.E-4
300             Velocity=Mflw/(Rho*A)
310             PRINT USING 160;Pcar;Pdrope;Mflw;Mflw*1000./453.5924;Rho;F;Re;Velocity
320         NEXT Pcar
330         PAUSE
340         Fric: !
350         SELECT Re
360         CASE <2300.
370             GOSUB Flam
380             F=Fr_lam
390         CASE 2300. TO 3000.
400             GOSUB Flam
410             GOSUB Fturb
420             F=.5*(Fr_lam+Fr_turb)
430         CASE 3000. TO 3.E+6
440             GOSUB Fturb
450             F=Fr_turb
460         CASE ELSE
470             BEEP
480             GOSUB Fturb
490             F=Fr_turb
500         END SELECT
510         RETURN
520     Flam: !
530     Fr_lam=64./Re
540     RETURN
550     Fturb: !
560     Fr_turb=.0056+.5*((Re^(-.32)))
570     RETURN
580     END

```

TABLE XI: Computer listing of program to calculate data presented in Tables V through X (MKS Units Version).

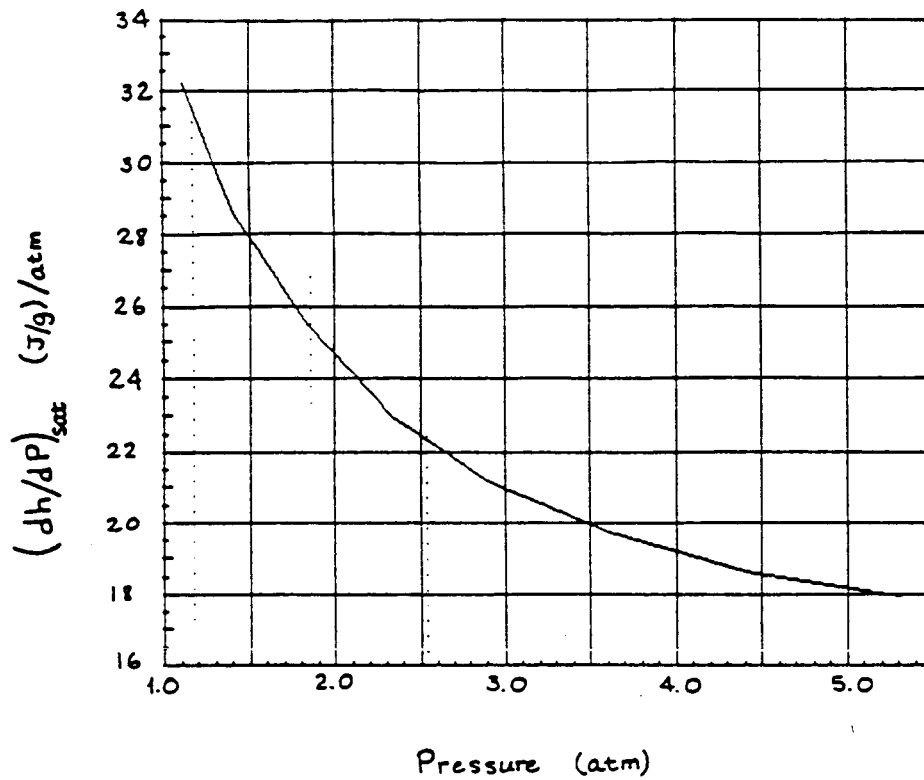


Fig. 1. $\left(\frac{dh}{dP}\right)_{sat}$ as a function of pressure.

P (atm)	dh/dP (J/g)/atm	
1.1165	32.189	
1.4230	28.447	-12.2071
1.8410	25.461	-07.1456
2.3400	22.970	-04.9901
2.9200	21.136	-03.1205
3.6135	19.715	-02.0723
4.4055	18.630	-01.3694
5.3115	17.938	-00.7645

Data Plotted in Fig. 1.

FIGURE 1: Rate of change of enthalpy as a function of pressure differential.

Finally, the external heat transfer must be equal to the sensible heating of the hydrogen. The equation for the sensible Heat Q_s of the hydrogen is:

$$M_g C_p(t) (t-30)$$

where M_g is the mass flow rate of hydrogen

$C_p(t)$ is the heat capacity of the hydrogen gas as a function of temperature

The following table summarizes the results. Most flows will be in the range of 1 to 1.5 lbm/sec. The temperature increase of the hydrogen for various lengths are given in Table XII.

Mass Flow Lbm/sec	Distance from Dewar Ft.	Temperature Rise °K
1.0	100	15.2
1.0	200	33.5
1.0	300	51.2
1.0	400	67.0
1.0	500	79.5
1.5	100	11.8
1.5	200	24.5
1.5	300	38.3
1.5	400	52.0
1.5	500	63.5

TABLE XII: Temperature increase of vented hydrogen due to external heat transfer from the ambient air.

The total flow rate of hydrogen vented comes from the boiloff from heating up the sphere, ullage displacement, and flashing. Ullage displacement has not been calculated yet. It may be determined by the mass flow rate of liquid into the dewar and using the density of the liquid, determining the volume displacement rate. Using the density of the vapor leaving the dewar and the volume displacement rate, the mass flow rate of vapor leaving the dewar due to displacement can be calculated and an equivalent SCFM found.

Dewar LH ₂ Level Gallons	Sphere Sensible Heat		SCFMx10 ³ Ullage	SCFMx10 ³ Flashing	Total Boil-off SCFMx10 ³
	Boil-off				
50,000	228		1.903	5.886	7.783
100,000	103		2.002	6.196	8.192
150,000	83		2.056	6.406	8.456
200,000	73		2.090	6.706	8.790
250,000	68		2.115	6.856	8.965
300,000	64		2.131	7.136	9.261
350,000	62		2.145	7.336	9.475
400,000	61		2.153	7.456	9.603
450,000	60		2.163	7.496	9.653
500,000	61		2.169	7.636	9.799
550,000	62		2.185	7.686	9.855
600,000	64		2.189	7.716	9.889
650,000	68		2.183	7.886	10.063
700,000	73		2.187	7.896	10.077
750,000	83		2.191	7.756	9.941
800,000	103		2.193	7.606	9.793

TABLE XIII: Shows the contribution of each of the terms to the boiloff for a dewar at 2.5 psig and line pressure of 22.5 psig.

REFERENCES

1. ASHRAE Handbook of Fundamentals, 1972 Edition.
2. Cryogenic Systems, Barron, McGraw Hill Series in Mechanical Engineering, 1966, p. 517.
3. Cryogenic Engineering, Scott, Van Nostrand, 1959, p. 306.
4. Convective Heat and Mass Transfer, McGraw Hill, 1966.
5. Handbook of Chemistry and Physics, 41st Edition.
6. Fundamentals of Classical Thermodynamics, Van Wylen, Gordon and Sonntag, John Wiley and Sons, Inc.
7. Technology and Use of Liquid Hydrogen, Chapter 11.
8. Experimental Techniques in Low Temperature Physics, White, Guy.K., p. 59.
9. Flow of Fluids through Valves, Fittings and Pipe, Technical Paper. No. 410, Crane Company, pp. A-24 and A-25.

STANDARD TITLE PAGE

1. Report No.		2. Government Accession No.		3. Recipient's Catalog No.	
4. Title and Subtitle Capture of Liquid Hydrogen Boiloff with Metal Hydride Absorbers				5. Report Date April 1984	
7. Author(s) M. J. Rosso, P.M. Golden				6. Performing Organization Code	
9. Performing Organization Name and Address Ergenics, Inc. Wykoff, New Jersey				8. Performing Organization Report No.	
12. Sponsoring Agency Name and Address National Aeronautics and Space Administration John F. Kennedy Space Center, FL				10. Work Unit No.	
				11. Contract or Grant No. NAS10-10625	
15. Abstract Standard operating procedure at the Kennedy Space Center (KSC) for the Space Shuttle Program requires the storage and transfer of substantial quantities of liquid hydrogen (LH ₂). Vaporized liquid, routinely lost during these transfer operations, is vented to the atmosphere or burned in the burn pond, and represents a significant fraction of the total hydrogen-fuel used for each launch. This report described a procedure which uses metal hydrides to capture some of this low pressure (less than 1 psig) hydrogen for subsequent reliquefaction. Of the five normally occurring sources of boil-off vapor the stream associated with the off-loading of liquid tankers during dewar refill was identified as the most cost effective and readily recoverable. The design, fabrication and testing of a proof-of-concept capture device, operating at a rate that is commensurate with the evolution of vapor by the target stream, is described. Liberation of the captures hydrogen gas as pressures greater than 15 psig at normal temperatures (typical liquefier compressor suction pressure) are also demonstrated. A payback time of less than three years is projected.				13. Type of Report and Period Covered Final Report of Study	
				14. Sponsoring Agency Code DD-MED	
16. Key Words Metal Hydrides, Absorption, Poisoning, Boiloff, Isotherm, Kinetics					
17. Bibliographic Control			18. Distribution Unclassified-Unlimited Subject Category 28		
19. Security Classif.(of this report) Unclassified		20. Security Classif.(of this page) Unclassified		21. No. of Pages 89	22. Price